to the plane of the four nitrogen atoms and the other molecule having these planes nearly parallel (dihedral angles 2.2 and 13.9°). The packing of the mesityl-substituted $As_2S_2N_4$ rings shows parallel planes of mesityl rings, whereas the phenyl substituted material shows no such regularity of orientation of the aromatic rings (Figures 3 and 4).

Acknowledgment. N.W.A. and E.M.H. gratefully acknowledge the assistance of a grant from NATO.

Registry No. $As_2S_2N_4C_{18}H_{22}$, 70369-31-2; $As_2S_2N_4C_{12}H_{10}$, 70369-32-3; $Me_3SiNSNSNSNSiMe_3$, 53380-71-5; $PhAsCl_2$, 696-28-6; $MeSAsCl_2$, 70369-33-4; $Me_3SiNSNSiMe_3$, 18156-25-7; PhAsCl(-NSNSiMe$_3$), 70369-34-5; PhAsCl(-NSNSNSNSiMe$_3$), 70369-35-6; MeSAsCl(-NSNSiMe$_3$), 70369-36-7; MeSAs(-NSNSiMe$_3$)$_2$, 70369-37-8; MeSAsCl(-NSNSNSNSiMe$_3$), 70369-38-9; $PhAsS_3N_4$, 70369-39-0; $MeSAsS_3N_4$, 70369-40-3.

Supplementary Material Available: Observed and calculated structure amplitudes and anisotropic thermal parameters (31 pages). Ordering information is given on any current masthead page.

References and Notes

(1) (a) University of Warwick. (b) To whom correspondence should be addressed at the Department of Biochemistry, University of Georgia, Athens, GA 30602. (c) I.B.M. Research Laboratory.
(2) Greene, R. L.; Street, G. B.; Suter, L. *J. Phys. Rev. Lett.* **1975**, *34*, 577.
(3) Street, G. B.; Gill, W. D.; Geiss, R. H.; Greene, R. L.; Mayerle, J. J. *J. Chem. Soc., Chem. Commun.* **1977**, 407.
(4) Kuyper, J.; Street, G. B. *J. Am. Chem. Soc.* **1977**, *99*, 7848.
(5) Alcock, N. W. "Crystallographic Computing", Ahmed, F., Ed.; Munksgaard: Copenhagen, 1970; p 271.
(6) "International Tables for Crystallography"; Kynoch Press: Birmingham, England, 1974; Vol. IV.
(7) Cromer, D.; Mann, J. *Acta Crystallogr., Sect. A*, **1968**, *24*, 321.
(8) Stewart, J. M. "The X-Ray System, Technical Report TR-446 of the Computer Science Center"; University of Maryland, College Park, MD, 1976.
(9) Sharma, B. D.; Donohue, J. *Acta Crystallogr.*, **1963**, *16*, 891.
(10) Bondi, A. *J. Phys. Chem.* **1964**, *68*, 441.
(11) Tobelko, K. I.; Zvonkova, Z. V.; Zhdanov, G. S. *Dokl. Akad. Nauk SSSR* **1954**, *96*, 749.
(12) Holt, E. M.; Holt, S. L.; Watson, K. J. *J. Chem. Soc., Chem. Commun.*, **1977**, 514.
(13) Weiss, J.; Eisenhuth, W. *Z. Anorg. Allg. Chem.* **1977**, *350*, 9.
(14) Hazell, A. C.; Hazell, R. G. *Acta Chem. Scand.* **1972**, *26*, 1987.
(15) Cordes, A. W.; Kruh, R.; Gordon, E. K. *Inorg. Chem.* **1965**, *4*, 681.
(16) Olsen, F. B.; Barrick, J. C. *Inorg. Chem.* **1973**, *12*, 1353.
(17) Holt, E. M.; Holt, S. L.; Watson, K. J. *J. Chem. Soc., Dalton Trans.* **1974**, 1357.
(18) Roesky, H. W.; Bowing, W. G.; Rayment, I.; Shearer, H. M. M. *J. Chem. Soc., Chem. Commun.* **1975**, 735.
(19) Holt, E. M.; Holt, S. L.; Watson, K. J. *J. Chem. Soc.* **1974**, 1990.
(20) Kirchhoff, W. H.; Wilson, E. B., Jr. *J. Am. Chem. Soc.* **1963**, *85*, 1726.
(21) Kirchhoff, W. H.; Wilson, E. B., Jr. *J. Am. Chem. Soc.* **1962**, *84*, 334.

Contribution from the Departments of Chemistry, Northwestern University, Evanston, Illinois 60201, and Faculty of Engineering Science, Osaka University, Toyonaka, Osaka, Japan 560

Cationic Binuclear Trihydride Complexes of Platinum. A Fluxional Behavior for Bridging and Terminal Hydrido Ligands. Crystal and Molecular Structure of $[Pt_2H_3\{(t\text{-Bu})_2P(CH_2)_3P(t\text{-Bu})_2\}_2][B(C_6H_5)_4]$

T. H. TULIP,[1a] T. YAMAGATA,[1b] T. YOSHIDA,[1b] R. D. WILSON,[1a] JAMES A. IBERS,*[1a] and SEI OTSUKA*[1b]

Received November 27, 1978

A series of complexes of bis(diphosphine)trihydridodiplatinum(II) cations have been prepared from the corresponding mononuclear *cis*-(diphosphine)dihydridoplatinum(II) or dimeric bis(diphosphine)diplatinum(0) compexes. These complexes are very stable. While their IR spectra are consistent with the presence of both terminal and bridging hydrido ligands, the NMR spectra are consistent with only one form of hydride coordination and show equivalence within the sets of H, P, and Pt atoms. These results suggest a rapid exchange of bridging and terminal hydrido ligands. The static molecular structure is proposed to involve one bridging and two terminal hydrido ligands. The complex $[Pt_2H_3\{(t\text{-Bu})_2P(CH_2)_3P(t\text{-Bu})_2\}_2][B(C_6H_5)_4]$ crystallizes in space group C_{2h}^5-$P2_1/c$ with four formula units in a cell of dimensions a = 19.41 (1) Å, b = 18.03 (1) Å, c = 21.51 (1) Å, and β = 120.57 (3)°. The complex is sensitive to X radiation as evidenced by its progressive decomposition during data collection. Three data subsets on different crystals were acquired and merged to yield a total of 3468 unique reflections having $F_o^2 > 3\sigma(F_o^2)$. Least-squares refinement, including anisotropic thermal parameters for Pt and P atoms but isotropic parameters for the other nonhydrogen atoms, led to final conventional agreement indices (on F) of R = 0.081 and R_w = 0.101. The hydrido ligands were not located, but their positions are inferred from the coordination geometries of the Pt atoms. The Pt–Pt separation is 2.768 (2) Å and the dihedral angle between the two P–Pt–P coordination planes is 89°. The spectral and structural details, as well as those of the fluxional process, are discussed and related to those of similar mono- and binuclear platinum complexes.

Interest in hydride complexes of the transition metals has grown steadily since the first report by Hieber and Leutert in 1931.[2-4] The synthetic, analytical (spectroscopic[5] and diffraction[6]), and theoretical challenges posed by these complexes, augmented by the recognition of their intimate involvement in many aspects of homogeneous catalysis,[7] have drawn ever-increasing attention during the past two decades. Most recently much of this interest has turned to polyhydride complexes, both mono- and polymetallic. Although a wide variety of monohydride complexes of Pt(II) are well-known,[8-10] dihydride species were not reported until recently.[11-17] Thermally and kinetically stable *trans*-dihydride complexes, *trans*-PtH_2L_2, have been prepared in which the auxiliary ligands, L, are sterically demanding tertiary phosphines.[11-15] We have previously described the synthesis of an analogous series of novel *cis*-dihydride complexes of Pt(II).[17] Their isolation was made possible by constraining the two phosphorus donor atoms to cis positions by their incorporation into a chelating diphosphine incapable of spanning trans coordination sites and by including bulky phosphine substituents which kinetically stabilize the *cis*-dihydride coordination.

Although polynuclear complexes incorporating bridging hydrido ligands are known for many of the transition metals, few examples have been reported for platinum, e.g., $Pt_2Y_2(\mu\text{-H})_2L_2$ [L = PCy_3 (Cy = cyclohexyl); Y = H, MR (M = Si, Ge; R = alkyl)].[18,19] In our continuing investigations into the chemistry of *cis*-dihydridoplatinum(II) and related dimeric Pt(0) complexes, we have discovered an interesting series of cationic trihydridodiplatinum complexes, $[Pt_2H_3(diphos)_2]X$ [(diphos) = $R_1R_2P(CH_2)_nPR_1R_2$ (n = 2, 3, R_1 = R_2 = t-Bu; n = 2, R_1 = Ph, R_2 = t-Bu); X = Cl, OMe, BPh_4], which could be prepared by a number of routes. The IR spectra of these complexes are consistent with the presence of both bridging and terminal hydrido ligands. However, ^1H and ^{31}P NMR

0020-1669/79/1318-2239$01.00/0

Table I. Physical Properties and Analytical Data

compd	compd no.	color	mp,[a] °C	anal., % C calcd	C found	H calcd	H found	Cl calcd	Cl found
$PtClH[(t\text{-}Bu)_2P(CH_2)_2P(t\text{-}Bu)_2]$	6	colorless	174	39.31	38.92	7.51	7.48	6.45	7.07
$[Pt_2H_3\{R(t\text{-}Bu)P(CH_2)_nPR(t\text{-}Bu)\}_2][B(C_6H_5)_4]$									
R = *t*-Bu, *n* = 3	2	colorless	225	54.06	53.60	7.83	7.77		
R = *t*-Bu, *n* = 2	1	colorless	>239	53.40	53.49	7.69	7.71		
R = Ph, *n* = 2	4	colorless	170	57.41	58.14	6.14	6.44		

[a] Under N_2, with decomposition.

Table II. Spectral Data of Complexes 1-6

				IR,[a] cm^{-1}		^1H NMR: *t*-Bu		^1H NMR: Pt-H			^{31}P NMR				
				ν_{PtH}	ν_{PtHPt}	δ[b]	$^3J_{PH}$, Hz	δ[b]	$^1J_{PtH}$, Hz	$^2J_{PH}$, Hz	δ[c]	$^1J_{PtP}$, Hz	$^2J_{PtP}$, Hz	$^3J_{PP}$, Hz	$^1J_{PtPt}$, Hz
$PtHCl[(t\text{-}Bu)_2P(CH_2)_2P(t\text{-}Bu)_2]$[d]	(6)			2013		1.30 d,[e,f] 1.37 d	13.8, 12.8	−3.88 dd	no[g]	199.5, 13.5					
$[Pt_2H_3\{R(t\text{-}Bu)P(CH_2)_nPR(t\text{-}Bu)\}_2]X$															
R	*n*	X	no.												
t-Bu	3	BPh_4	2	2045	ca. 1650	1.25 d[f]	13.5	−5.89 qq	395.7	37.9	49.4[f]	+3039.0	+168.0	6.8	840.2
t-Bu	3	OMe	3			1.13 d[h]	13.5	−5.90 qq	396.0	37.2					
t-Bu	2	BPh_4	1	2000	ca. 1650	1.26 d[f]	13.8	−3.85 qq	443.1	40.2	108.7[f]	+2946.2	+161.3	7.9	815.4
Ph	2	BPh_4	4	2010	ca. 1650	1.19 d[f]	15.7	−3.01 qq	467.4	40.2					
Ph	2	OMe	5			1.31 d[h]	12.6	−2.98 qq	456.9	41.9					

[a] Measured as Nujol mull. [b] Ppm downfield from Me_4Si. [c] Ppm downfield from H_3PO_4. [d] ν_{PtCl} = 285 cm^{-1}. [e] Abbreviations: d = doublet; q = quintet. [f] Measured in $CDCl_3$. [g] no, not observed. [h] Measured in toluene-d_8.

spectra exhibit resonances consistent with only one type of hydride coordination and indicate a rapid exchange among all hydrido ligands. Facile hydrido ligand equilibration of this type is documented for only a few transition-metal complexes.[18] During the interim since our initial discovery of these complexes, two reports concerning the isolation of similar $[Pt_2H_3(diphos)_2]$ cationic complexes have appeared.[20,21] In both cases exchange of hydrido ligands is also observed.

A synthesis of spectroscopic and diffraction studies promised to answer a number of questions arising from our initial observations concerning these trihydridodiplatinum cations, e.g.: (1) What is the static molecular structure consistent with the IR data? (2) By what mechanism is the rapid hydride scrambling accomplished? (3) What is the rationale for the facile formation of these complexes from the *cis*-PtH_2(diphos) and binuclear Pt_2(diphos)$_2$ complexes? With these objectives in mind we undertook these studies, the results of which are reported herein.

Experimental Section

^1H and $^{31}P\{^1H\}$ NMR spectra were recorded on JEOL JNM FX100 or NM-100 and Varian CFT-20 spectrometers, respectively. $^{31}P\{^1H\}$ spectra were recorded at 32.199 MHz and ^{31}P chemical shifts are reported in parts per million downfield from external 85% H_3PO_4. IR spectra were obtained by using an Hitachi Perkin-Elmer 225 instrument and conductivities were measured with a Yanagimoto conductivity outfit, Model MY-7. Platinum starting materials were prepared as previously described.[17] Reactions involving Pt(0) complexes were carried out under an N_2 atmosphere. Tables I and II present physical-analytical and spectral data, respectively, for the complexes reported.

Bis(diphos)trihydridodiplatinum Cations. $[Pt_2H_3\{(t\text{-}Bu)_2P(CH_2)_2P(t\text{-}Bu)_2\}_2][BPh_4]$ (1). Method A. [1,2-Bis(di-*tert*-butylphosphino)ethane]dihydridoplatinum (**7**) (0.134 g, 0.26 mmol) was dissolved in toluene (3 mL) containing 0.3 mL of $CHCl_3$. Colorless crystals formed within 2 h at ambient temperature. VPC analysis (Apiezon Grease L, 1.4 m, 50 °C) of the supernatant solution indicated production of CH_2Cl_2. The mixture was concentrated and the resulting solid extracted with 5 mL of EtOH and subsequently filtered. The EtOH-insoluble crystalline residue was identified as $PtCl_2[(t\text{-}Bu)_2P(CH_2)_2P(t\text{-}Bu)_2]$ (0.039 g, 26%) by comparison of its IR spectrum with that of an authentic sample. The ethanol filtrate was treated with an excess of $NaBPh_4$, resulting in the precipitation of colorless crystals of **1** which were washed successively with H_2O and EtOH and dried in vacuo (0.117 g, 67%).

Method B. A mixture of **7** (0.094 g, 0.18 mmol) and [1,2-bis(di-*tert*-butylphosphino)ethane]hydridochloroplatinum (**6**) (vide infra), (0.100 g, 0.18 mmol) was stirred in toluene (15 mL) at room temperature for 24 h. The mixture was concentrated, extracted with EtOH (10 mL), and filtered to remove unreacted starting materials. Subsequent addition of $NaBPh_4$ to this filtrate yielded **1** (0.133 g, 55%).

$[Pt_2H_3\{(t\text{-}Bu)_2P(CH_2)_3P(t\text{-}Bu)_2\}_2]X$ [X = BPh_4 (2), OMe (3)]. Compound **2** was prepared from [1,3-bis(di-*tert*-butylphosphino)propane]dihydridoplatinum (**8**) and $CHCl_3$ by method A (91%). In this case, the formation of $PtCl_2[(t\text{-}Bu)_2P(CH_2)_3P(t\text{-}Bu)_2]$ was not detected.

Method C. In an NMR tube 0.031 g (0.03 mmol) of $Pt_2[(t\text{-}Bu)_2P(CH_2)_3P(t\text{-}Bu)_2]_2$ (**10**) was dissolved in 0.5 mL of toluene-d_8 and the solution treated with MeOH (0.05 mL). The resulting red solution gradually changed to pale brown in the course of 3 days at ambient temperature. ^1H NMR spectra indicate the formation of the methoxide complex **3**. Addition of $NaBPh_4$ to an ethanolic solution of the concentrated residue yielded the BPh_4 salt **2** quantitatively.

$[Pt_2H_3\{Ph(t\text{-}Bu)P(CH_2)_2PPh(t\text{-}Bu)\}_2]X$ [X = BPh_4 (4), OMe (5)]. These two complexes were prepared by method C. The compound $Pt_2[Ph(t\text{-}Bu)P(CH_2)_2PPh(t\text{-}Bu)]_2$ was prepared in situ from the corresponding *cis*-dihydride complex **9**.[17] The tetraphenylborate salt **4** was obtained in 88% yield as colorless crystals.

Thermal Reaction of 5. A toluene-d_8 solution of **5**, prepared as described above from **9** (0.076 g, 0.137 mmol), was heated at 65 °C for 15 min. Concentration of the resulting solution yielded yellow crystals which were identified (^1H NMR, IR) as the starting *cis*-dihydride complex **9**.

$PtClH[(t\text{-}Bu)_2P(CH_2)_2P(t\text{-}Bu)_2]$ (6). A total of 1.03 mL of a 1 M aqeuous solution of KOH was added to a suspension of $PtCl_2$-

Table III. Summary of Crystal Data and Intensity Collection

compd	$[Pt_2H_3\{(t\text{-Bu})_2P(CH_2)_3P(t\text{-Bu})_2\}_2]\text{-}[B(C_6H_5)_4]$
formula	$C_{62}H_{107}BP_4Pt_2$
fw	1377.43
a, Å	19.41 (1)
b, Å	18.03 (1)
c, Å	21.51 (1)
β, deg	120.57 (3)
V, Å^3	6482
Z	4
density, g cm^{-3}	1.41 (calcd) 1.41 (1) (obsd)
space group	$C_{2h}{}^5\text{-}P2_1/c$
cryst dimens, mm	(1)[a] 0.07 × 0.13 × 0.59 (2) 0.06 × 0.09 × 0.55 (3) 0.05 × 0.12 × 0.58
cryst shape	flattened pseudohexagonal needles with faces of the forms {100}, {001}, {011}
crystal vol, mm^3	(1) 0.0061 (2) 0.0020 (3) 0.0040
temp, °C	21.2 ± 0.6
radiation	Cu Kα (λ(Cu Kα$_1$) 1.540 562 Å) prefiltered with 1-mil Ni foil
μ, cm^{-1}	92.3
transmission factors	(1) 0.243–0.567 (2) 0.528–0.620 (3) 0.267–0.602
receiving aperture	(1) 6.1 × 3.2 mm (2) 6.0 × 3.0 mm (3) 6.0 × 3.2 mm } 30 cm from cryst
takeoff angle, deg	(1) 4.5 (2) 4.0 (3) 4.5
scan speed	2.0° min^{-1} in 2θ
scan range	1.0° below Kα$_1$ to 1.0° above Kα$_2$
bkgd counts	(1) and (2) 10 s, single rescan for observn with $I < 3\sigma(I)$ (see text) (3) 20 s, single rescan for observn with $I < 3\sigma(I)$
2θ limits, deg	(1) 3.0–60.0 (2) 60.0–67.0 (3) 67.0–84.0
observns	$h,k,\pm l$
total no. of observns	4832
no. of unique data, $F_o{}^2 > 3\sigma(F_o{}^2)$	3468
final no. of variables	261
R	0.081
R_w	0.101
error in observn of unit wt	4.7 electrons

[a] (1), (2), and (3) refer to the data from the three different crystals.

$[(t\text{-Bu})_2P(CH_2)_2P(t\text{-Bu})_2]$ (0.60 g, 1.03 mmol) in 30 mL of EtOH and the mixture was heated at reflux for 0.5 h to give a clear, pale brown solution. Extraction of the concentrated mixture with hot toluene resulted in the formation of colorless crystals (0.23 g, 41%), upon addition of *n*-hexane.

Collection and Reduction of the X-ray Data. Crystals of $[Pt_2H_3\{(t\text{-Bu})_2P(CH_2)_3P(t\text{-Bu})_2\}_2][BPh_4]$ suitable for diffraction were obtained by slowly cooling a 1:1 chloroform–toluene solution. Preliminary photographic data of a crystal mounted in air revealed that the material belongs to the monoclinic system (Laue symmetry $2/m$). Systematic extinctions ($h0l$, $l = 2n + 1$; $0k0$, $k = 2n + 1$) characteristic of the space group $C_{2h}{}^5\text{-}P2_1/c$ were observed.

Cell constants were obtained by the least-squares refinement of 15 reflections hand-centered on a FACS-I diffractometer.[22] These reflections were generated with a narrow source and chosen from diverse regions of reciprocal space [$40.2° \leq 2\theta(\text{Cu K}\alpha_1) \leq 48.9°$]. These cell dimensions and other crystallographic data are compiled in Table III.

Intensity data were collected in shells of 2θ by using the θ–2θ technique. Background counts were measured at both ends of the scan range with both the counter and crystal held stationary. If the observed peak intensity was less than 3σ, as defined by the background counting statistics, the reflection was rescanned and each background recounted for twice its original time. The results of the two scans and two backgrounds were then combined.

The intensities of six standard reflections were measured every 100 reflections. These standard intensities varied monotonically during the course of data collection as a result of crystal decomposition. Thus data collection was terminated at $2\theta = 60.0°$, at which time the standard reflections had decreased an average of 8%. The relative changes in intensities for the six standard reflections varied markedly. In fact, one of the reflections (002) actually increased in intensity. A facile ambient light photolysis of similar trihydridodiplatinum cationic complexes with bridging diphosphine ligands has been noted by Brown and co-workers.[20] We felt that the most probable decomposition pathway involves loss of H_2. Therefore a second crystal was chosen and sealed in a glass capillary under an atmosphere of H_2. This second crystal was treated similarly to the first sample and data were collected in the shell $60.0° < 2\theta(\text{Cu K}\alpha_1) \leq 67.0°$. The six standard reflections, with an average decay of 7%, showed variations in intensities similar to those observed for the first crystal. This encapsulated crystal was then replaced by a third, fiber-mounted crystal and a final subset of data was collected in the range of $67.0° < 2\theta(\text{Cu K}\alpha_1) \leq 84.0°$. Average intensity loss in the six standards during this period of irradiation was 7%. The data were processed as previously described by using a p value of 0.04.[23] After processing of the data, only 3468 unique reflections having $F_o{}^2 > 3\sigma(F_o{}^2)$ were used in subsequent calculations. Each data subset was corrected for absorption,[24] brought to an approximately common scale, and merged. Separate scale factors were used in ensuing calculations. Attempts to correct for decomposition by using models derived from the observed changes in the standard reflections were unsuccessful.

Solution and Refinement of the Structure. The platinum atoms were easily located in a three-dimensional, original-removed, sharpened Patterson synthesis. After an initial refinement of the three separate scale factors in which the platinum atom positions were not varied, the positions of the nonhydrogen atoms were obtained through the usual combination of least-squares refinements and difference Fourier syntheses. The quantity minimized was $\sum w(|F_o| - |F_c|)^2$ where $w = 4F_o{}^2/\sigma^2(F_o{}^2)$ and $|F_o|$ and $|F_c|$ are the observed and calculated structure amplitudes, respectively. The agreement indices for the F_o refinement are $R = \sum ||F_o| - |F_c||/\sum |F_o|$ and $R_w = (\sum w(|F_o| - |F_c|)^2/\sum wF_o{}^2)^{1/2}$. Atomic scattering factors for the nonhydrogen atoms were taken from the tabulation of Cromer and Waber[25] whereas the hydrogen scattering factors used were those of Stewart et al.[26] Anomalous dispersion terms were included in F_c.[27] The phenyl rings of the tetraphenylborate anion were treated as rigid groups[28] and restricted to their known geometry ($6/mmm$ symmetry, d(C–C) = 1.395 Å). Initially only a group thermal parameter was refined although in the final stages of refinement each of the group atoms was assigned an individual isotropic thermal parameter.

Isotropic refinement of the nonhydrogen atoms resulted in agreement indices of 0.144 and 0.170 for R and R_w. The ensuing full-matrix refinement, in which each of the nongroup nonhydrogen atoms was allowed to vibrate anisotropically while the group carbon atoms of the anion were restricted to isotropic vibration, was unsuccessful in that the thermal parameters of three of the carbon atoms became nonpositive definite. Even so, the R index was 0.082 and on an ensuing difference Fourier map the positions of 65 of the 72 hydrogen atoms of the methyl groups were clear. These positions, as well as those of the 7 remaining hydrogen atoms on the methyl groups, the 12 hydrogen atoms of the methylene groups, and the 20 hydrogen atoms of the phenyl groups, were idealized assuming the appropriate geometries and a C–H distance of 0.95 Å. Each hydrogen atom was assigned an isotropic thermal parameter of 1.0 Å^2 larger than that of the carbon atom to which it is attached. The contributions of these hydrogen atoms to the total scattering was held constant thereafter. In a final cycle of least-squares refinement, all nonhydrogen atoms were restricted to isotropic refinement save for the platinum and phosphorus atoms, which were refined anisotropically. This refinement converged to agreement indices of 0.081 and 0.101 and to an error in an observation of unit weight of 4.7 electrons.

An analysis of $\sum w(|F_o| - |F_c|)^2$ as a function of $|F_o|$, setting angles, and Miller indices reveals no unexpected trends. Thus we feel that the unsatisfactory results of the attempted anisotropic refinement arise from inadequacies in the data sets which in turn derive from crystal decomposition. A difference Fourier map revealed the presence of

Table IV. Positional and Thermal Parameters for the Nongroup Atoms of $[Pt_2H_3\{(t\text{-}Bu)_2P(CH_2)_3P(t\text{-}Bu)_2\}_2][B(C_6H_5)_4]$

ATOM	X[a]	Y	Z	B11 OR B,Å^2[b]	B22	B33	B12	B13	B23
PT(1)	0.300487(66)	0.212370(65)	0.281891(69)	23.05(85)	51.65(76)	33.61(76)	-0.31(44)	18.07(54)	1.27(45)
PT(2)	0.141779(65)	0.197765(67)	0.243924(66)	20.81(85)	57.08(80)	29.29(72)	-1.34(44)	15.20(53)	-4.84(46)
P(1)	0.37272(42)	0.11004(39)	0.27834(42)	33.1(36)	42.2(32)	40.8(35)	4.7(27)	22.5(30)	8.6(27)
P(2)	0.38318(40)	0.30456(38)	0.28742(42)	26.0(33)	43.3(32)	36.0(32)	1.6(26)	18.8(28)	-0.6(27)
P(3)	0.11620(41)	0.19547(40)	0.33955(40)	29.7(35)	58.4(37)	30.5(31)	-4.0(27)	20.6(28)	-4.3(27)
P(4)	0.01498(41)	0.20512(37)	0.15069(40)	25.5(33)	47.2(32)	31.5(31)	-0.8(25)	16.8(27)	-2.9(26)
B	-0.2813(18)	0.2044(16)	0.2684(17)	4.94(75)					
C(1)	0.4614(19)	0.1360(18)	0.2725(18)	6.79(88)					
C(2)	0.4976(19)	0.1997(17)	0.3004(17)	9.26(82)					
C(3)	0.4728(18)	0.2752(16)	0.2825(17)	5.38(78)					
C(4)	0.0145(19)	0.1951(15)	0.3111(18)	7.07(78)					
C(5)	-0.0464(21)	0.2096(16)	0.2440(21)	12.00(91)					
C(6)	-0.0658(18)	0.2041(14)	0.1704(17)	6.15(76)					
C(111)	0.4165(18)	0.0524(16)	0.3636(17)	6.60(76)					
C(112)	0.4887(21)	0.0038(17)	0.3736(19)	9.66(94)					
C(113)	0.3573(20)	-0.0024(18)	0.3638(19)	7.58(92)					
C(114)	0.4454(18)	0.1037(15)	0.4249(17)	7.71(79)					
C(121)	0.3121(19)	0.0550(17)	0.1908(17)	6.94(82)					
C(122)	0.3593(20)	-0.0102(18)	0.1843(19)	8.14(93)					
C(123)	0.2373(20)	0.0160(17)	0.1882(19)	8.49(93)					
C(124)	0.2855(19)	0.1060(17)	0.1278(18)	6.71(88)					
C(211)	0.4215(20)	0.3603(18)	0.3699(19)	6.70(87)					
C(212)	0.3619(22)	0.3940(19)	0.3813(20)	8.3(10)					
C(213)	0.4800(21)	0.4219(18)	0.3775(19)	10.28(96)					
C(214)	0.4734(24)	0.3088(19)	0.4338(23)	10.5(11)					
C(221)	0.3280(19)	0.3676(17)	0.2080(18)	6.47(79)					
C(222)	0.2921(20)	0.3154(17)	0.1422(19)	8.00(90)					
C(223)	0.2592(19)	0.4055(17)	0.2101(18)	6.75(87)					
C(224)	0.3801(20)	0.4212(17)	0.1953(19)	9.88(92)					
C(311)	0.1520(19)	0.2807(15)	0.3961(18)	5.43(78)					
C(312)	0.1320(19)	0.3490(17)	0.3485(18)	7.42(86)					
C(313)	0.2419(21)	0.2832(16)	0.4440(19)	8.27(92)					
C(314)	0.1181(21)	0.2915(16)	0.4452(20)	8.74(94)					
C(321)	0.1499(18)	0.1088(16)	0.3951(17)	5.81(77)					
C(322)	0.1171(18)	0.0969(16)	0.4490(17)	7.13(83)					
C(323)	0.1223(19)	0.0474(17)	0.3425(18)	9.17(89)					
C(324)	0.2415(20)	0.1018(17)	0.4380(19)	8.86(94)					
C(411)	-0.0040(16)	0.2929(13)	0.0975(15)	3.98(60)					
C(412)	-0.0836(22)	0.3019(17)	0.0359(20)	10.12(97)					
C(413)	0.0549(25)	0.3066(18)	0.0726(23)	8.8(11)					
C(414)	0.0127(21)	0.3594(19)	0.1466(20)	10.0(10)					
C(421)	-0.0122(15)	0.1213(13)	0.0907(14)	3.83(62)					
C(422)	0.0322(18)	0.1177(16)	0.0480(17)	8.19(85)					
C(423)	0.0087(20)	0.0556(17)	0.1345(19)	8.24(92)					
C(424)	-0.0996(19)	0.1151(16)	0.0346(18)	8.06(86)					

[a] ESTIMATED STANDARD DEVIATIONS IN THE LEAST SIGNIFICANT FIGURE(S) ARE GIVEN IN PARENTHESES IN THIS AND ALL SUBSEQUENT TABLES. [b] THE FORM OF THE ANISOTROPIC THERMAL ELLIPSOID IS: $\exp[-(B11h^2+B22k^2+B33l^2+2B12hk+2B13hl+2B23kl)]$. THE QUANTITIES GIVEN IN THE TABLE ARE THE THERMAL COEFFICIENTS $\times 10^4$.

a number of areas of residual electron density, the two greatest of which correspond to approximately 3 e Å^{-3} and are about 3.5 Å from the platinum atoms. The 12 highest residual peaks (≥ 0.86 e Å^{-3}) are arrayed in two lines, each of which passes through one of the platinum atom positions and is approximately parallel to *b*. It is interesting that both lines of residual density lie in a plane parallel to the *ab* plane and thus may be related to the increase in the intensity of the 002 reflection with X-ray exposure. None of the residual peak positions correspond to chemically reasonable sites for terminal or bridging hydrido ligands.

The final positional and thermal parameters of the nonhydrogen atoms appear in Tables IV and V. Idealized hydrogen atom positions are compiled in Table VI.[29] Listings of the observed and calculated structure amplitudes and the root-mean-square amplitudes of vibration (Table VII) are available.[29]

Results

Syntheses. When the *cis*-dihydride complex $PtH_2[(t\text{-}Bu)_2P(CH_2)_2P(t\text{-}Bu)_2]$ is treated with $CHCl_3$ in toluene at room temperature, the reaction mixture yields two products, EtOH-insoluble $PtCl_2[(t\text{-}Bu)_2P(CH_2)_2P(t\text{-}Bu)_2]$ and EtOH-soluble $[Pt_2H_3\{(t\text{-}Bu)_2P(CH_2)_2P(t\text{-}Bu)_2\}_2]Cl$. A gas chromatographic analysis of the final filtrate confirms the presence of CH_2Cl_2. Addition of $NaBPh_4$ to an EtOH solution of the second product readily gives in high yield the metathesis product $[Pt_2H_3\{(t\text{-}Bu)_2P(CH_2)_2P(t\text{-}Bu)_2\}_2][BPh_4]$ (**1**). The ionic nature of **1** was established from its equivalent conductance ($\Lambda = 17.2\ \Omega^{-1}$ cm^2 mol^{-1} in nitrobenzene). The diphosphinopropane analogue $[Pt_2H_3\{(t\text{-}Bu)_2P(CH_2)_3P(t\text{-}Bu)_2\}_2][BPh_4]$ (**2**) is obtained quantitatively by a similar reaction of $PtH_2[(t\text{-}Bu)_2P(CH_2)_3P(t\text{-}Bu)_2]$ with $CHCl_3$ followed by addition of $NaBPh_4$. Interestingly, no dichloro species, $PtCl_2[(t\text{-}Bu)_2P(CH_2)_3P(t\text{-}Bu)_2]$, is detected in this case. In an alternative synthesis we found that **1** could be prepared by combining equimolar amounts of $PtH_2[(t\text{-}Bu)_2P(CH_2)_2P(t\text{-}Bu)_2]$ and $PtClH[(t\text{-}Bu)_2P(CH_2)_2P(t\text{-}Bu)_2]$ in toluene at ambient temperatures. This result suggests that the formation of cationic trihydride complexes from the reaction of $CHCl_3$ with the corresponding *cis*-dihydride species occurs via incipient formation of the hydridochloro compounds, eq 1 and 2.

$$PtH_2(\text{diphos}) + CHCl_3 \rightarrow PtClH(\text{diphos}) + CH_2Cl_2 \quad (1)$$

$$PtH_2(\text{diphos}) + PtClH(\text{diphos}) \rightarrow [Pt_2H_3(\text{diphos})_2]Cl \quad (2)$$

Table V. Derived Parameters for the Rigid-Group Atoms of $[Pt_2H_3\{(t\text{-Bu})_2P(CH_2)_3P(t\text{-Bu})_2\}_2][B(C_6H_5)_4]$

ATOM	X	Y	Z	B, Å^2	ATOM	X	Y	Z	B, Å^2
C 11	-0.37585(82)	0.2070(11)	0.20242(93)	4.83(67)	C 31	-0.2322(10)	0.13185(81)	0.2596(11)	5.10(64)
C 12	-0.4185(11)	0.14100(76)	0.1761(10)	5.23(69)	C 32	-0.1671(12)	0.1024(10)	0.32162(79)	6.15(73)
C 13	-0.4992(11)	0.14286(82)	0.1225(11)	6.33(76)	C 33	-0.12033(91)	0.0472(10)	0.31577(97)	6.98(80)
C 14	-0.53721(84)	0.2107(11)	0.09519(95)	6.47(78)	C 34	-0.1387(11)	0.02147(86)	0.2479(13)	6.67(79)
C 15	-0.4945(12)	0.27672(80)	0.1215(11)	7.21(82)	C 35	-0.2039(13)	0.0509(11)	0.18582(88)	7.42(89)
C 16	-0.4139(12)	0.27486(78)	0.1751(11)	6.03(75)	C 36	-0.25065(92)	0.1061(10)	0.19167(85)	6.24(72)
C 21	-0.22749(96)	0.27660(75)	0.2645(11)	5.51(68)	C 41	-0.2867(11)	0.2046(11)	0.34335(87)	4.77(65)
C 22	-0.24261(89)	0.30408(96)	0.19808(80)	5.09(67)	C 42	-0.2896(11)	0.13684(79)	0.3732(11)	5.87(72)
C 23	-0.1939(12)	0.35947(98)	0.19559(82)	6.55(80)	C 43	-0.2977(12)	0.13524(87)	0.4340(11)	7.96(84)
C 24	-0.1300(10)	0.38737(80)	0.2595(11)	5.56(65)	C 44	-0.3028(12)	0.2014(13)	0.46503(91)	7.62(90)
C 25	-0.11492(87)	0.35989(98)	0.32591(85)	6.43(74)	C 45	-0.2999(12)	0.26917(89)	0.4352(11)	6.83(79)
C 26	-0.1636(11)	0.30451(96)	0.32840(78)	5.26(68)	C 46	-0.2918(11)	0.27078(77)	0.3744(11)	5.28(72)

RIGID GROUP PARAMETERS

GROUP	x_c, A	y_c	z_c	DELTA, B	EPSILON	ETA
GRP 1	-0.45653(79)	0.20886(65)	0.14881(69)	-0.032(12)	-3.169(11)	0.259(12)
GRP 2	-0.17876(66)	0.33199(57)	0.26200(68)	-1.565(20)	-2.148(11)	0.778(19)
GRP 3	-0.18549(70)	0.07666(62)	0.25372(72)	1.523(21)	2.188(12)	0.815(20)
GRP 4	-0.29475(68)	0.20301(66)	0.40419(73)	0.015(11)	-3.122(13)	-1.474(11)

A x_c, y_c, AND z_c ARE THE FRACTIONAL COORDINATES OF THE ORIGIN OF THE RIGID GROUP. B THE RIGID GROUP ORIENTATION ANGLES DELTA, EPSILON, AND ETA (RADIANS) HAVE BEEN DEFINED PREVIOUSLY: S.J. LA PLACA AND J.A. IBERS, ACTA CRYSTALLOGR., 18, 511 (1965).

Cationic trihydridodiplatinum complexes are also obtained by oxidative addition of MeOH to the dimeric Pt(0) complexes reported previously.[17] Thus a toluene solution of $Pt_2[(t\text{-Bu})_2P(CH_2)_3P(t\text{-Bu})_2]_2$ reacts readily with MeOH to give **3**. The in situ formation of $Pt_2[Ph(t\text{-Bu})P(CH_2)_2PPh(t\text{-Bu})]_2$ by thermal dehydrogenation of the corresponding *cis*-dihydride complex, followed by reaction with MeOH, yields an analogous binuclear cation. These results are explained in a scheme, eq 3 and 4, similar to that invoked above. Oxidative addition of

$$^1/_2Pt_2(diphos)_2 + CH_3OH \rightarrow PtH(OCH_3)(diphos) \rightarrow PtH_2(diphos) + CH_2O \quad (3)$$

$$PtH_2(diphos) + PtH(OCH_3)(diphos) \rightarrow [Pt_2H_3(diphos)_2][OCH_3] \quad (4)$$

MeOH to the Pt(0) complex would yield a hydridomethoxy complex which upon reaction with a *cis*-dihydride species forms a trihydridodiplatinum cation. In this case the dihydride complex could result from β-elimination of the hydridomethoxy complex with concomitant loss of formaldehyde. A similar dehydrogenation of methanol has been observed with PtL_2, where L is a bulky tertiary phosphine.[12] Further corroboration derives from the observation that gentle heating of **5** yields 2 equiv of the corresponding *cis*-dihydride, $PtH_2[Ph(t\text{-Bu})P(CH_2)_2PPh(t\text{-Bu})]$, presumably via a second β-elimination reaction.

All cationic trihydridodiplatinum complexes reported here are air stable in both solution and the solid state. They form colorless crystals which are soluble in polar solvents. Unlike the case for the dppm-bridged binuclear trihydride cations (dppm = bis(diphenylphosphino)methane),[20] which are sensitive to room light, we have observed no photodecomposition under normal conditions. However, as mentioned above, the crystals are decomposed by X radiation.

Spectra. The infrared spectra of complexes **1**, **2**, and **4**, measured both in solution and in the solid state, show intense absorptions between 2000 and 2050 cm^{-1} (Table II), attributable to the Pt–H(terminal) stretching mode ν_{Pt-H}. We ascribe broad bands observed at approximately 1650 cm^{-1} in the solid-state spectra (Nujol mulls) of these complexes to $\nu_{Pt-H-Pt}$.[19] The ^{1}H NMR spectra of the binuclear trihydride cations exhibit *tert*-butyl resonances as doublets ($^3J_{PH}$ = 12.6–15.7 Hz) centered at δ 1.13–1.26 (Table II), which indicate the equivalence of all *tert*-butyl groups. Note the lack

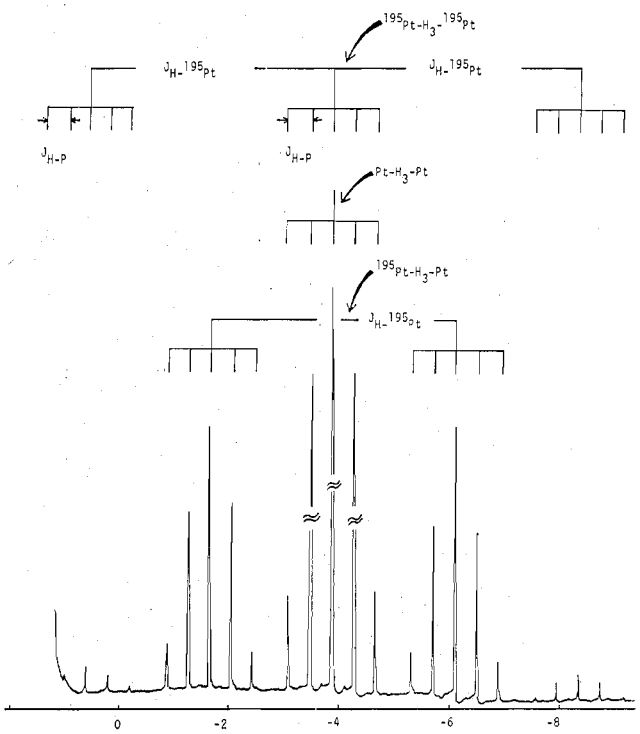

Figure 1. The hydride region of the ^{1}H NMR spectrum of **1**, $[Pt_2H_3\{(t\text{-Bu})_2P(CH_2)_2P(t\text{-Bu})_2\}_2][BPh_4]$. The scale is in ppm upfield from Me_4Si. A portion of the low-field quintet is obscured by the *t*-Bu resonance. The proposed coupling scheme is also shown.

of virtual coupling in contrast with the second-order spectrum observed for the *tert*-butyl resonance of $Pt_2[(t\text{-Bu})_2P(CH_2)_3P(t\text{-Bu})_2]_2$ (**10**).[17] This is indicative of weaker Pt–P and Pt–Pt bonding in these dimeric Pt(II) species compared with that in complex **10**. The absence of additive ($^3J_{PH} + {}^5J_{PH}$) coupling, which would result in a virtual triplet pattern, indicates cis chelation, rather than binuclear bridging, for the bulky diphosphines used.

The hydride resonances of complexes **1**–**5** are observed as quintets of quintets centered at δ −3.0 to −5.9 (Table II). Figure 1 displays the hydride spectrum of complex **1**. Part of the lowest field quintet signals were obscured by the *tert*-butyl doublet. A search of the high-field region up to δ

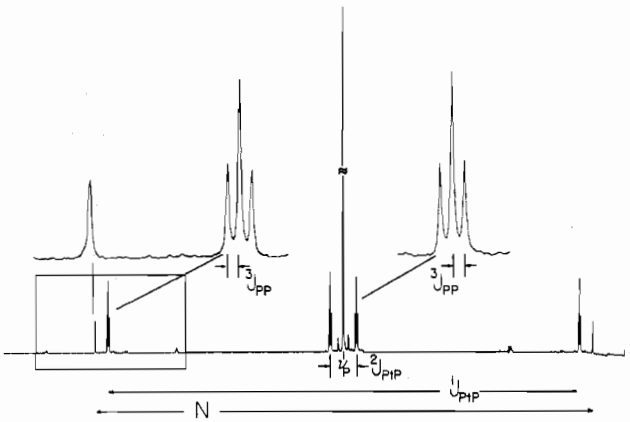

Figure 2. The $^{31}P\{^1H\}$ NMR spectrum of **2**, $[Pt_2H_3\{(t\text{-}Bu)_2P(CH_2)_3P(t\text{-}Bu)_2\}_2][BPh_4]$. H_0 increases to the right. The couplings, as explained in the text, are included ($N = {}^1J_{PtP} + {}^2J_{PtP}$) and smaller peaks have been expanded for clarity. The width of the box at the left corresponds to 1000 Hz. An enlargement of this box is shown in Figure 3.

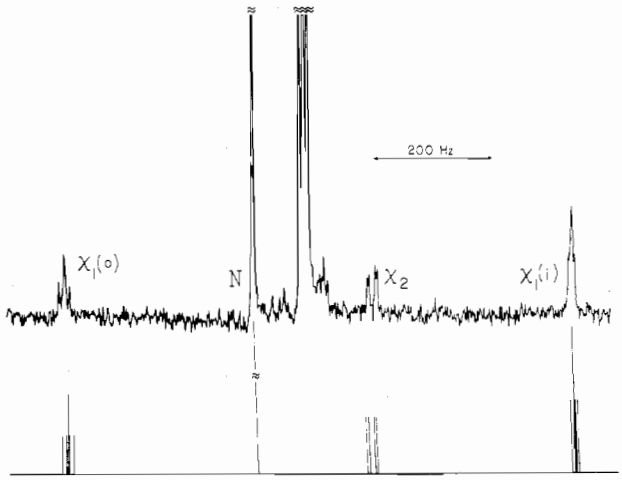

Figure 3. An expanded portion of the $^{31}P\{^1H\}$ NMR spectrum of **2** showing the fine structure arising from the $A_2A_2'XX'$ spin system of the $^{195}Pt_2$ isotopomer. H_0 increases to the right. The simulated spectrum of the $A_2A_2'XX'$ system is also included for comparison. The large central triplet which has no counterpart in the simulated spectrum arises from the $A_2A_2'X$ spectrum of the ^{195}Pt–Pt binuclear combination.

−25 failed to reveal additional hydride resonances. A similar result has been reported for $[Pt_2H_3(dppe)_2][BF_4]$ (dppe = bis(diphenylphosphino)ethane).[21] We interpret these data to indicate equivalence within the sets of three hydrido ligands, four phosphorus atoms, and two platinum atoms. The observed spectra arise from the superposition of three subspectra which emerge from the three possible isotopomeric combination of platinum atoms having different nuclear spins. The ^{195}Pt isotope has a natural abundance of 33.8% and is the only significant Pt isotope with nonzero nuclear spin ($I(^{195}Pt) = {}^1/_2$). This gives rise to three possible combinations in a binuclear complex: Pt–Pt, ^{195}Pt–Pt, and ^{195}Pt–^{195}Pt, the relative populations of which are approximately 4:4:1. The species Pt–H_3–Pt produces only a binomial quintet centered at ν_H arising from coupling $^2J_{PH}$ to four chemically and magnetically equivalent phosphorus nuclei. The binuclear complex containing only one ^{195}Pt nucleus gives rise to a 1:1 $^1J_{PtH}$ doublet about ν_H, each line of which is split into a $^2J_{PH}$ quintet. Interestingly, this quintet structure is not affected by the magnetic inequivalence of the phosphorus atoms, only two of which are bound to a ^{195}Pt nucleus. The spectrum of the third isotopomer ^{195}Pt–H_3–^{195}Pt exhibits a $^1J_{PtH}$ binomial triplet arising from identical interaction with two equivalent ^{195}Pt nuclei, with $^1J_{PtH}$ equal to that observed in the ^{195}Pt–H_3–Pt spectrum. Again, each of the triplet bands is split into a quintet by four equivalent P nuclei. The sum of the three subspectra should consist of five equally spaced quintets, separated by ${}^1/_2({}^1J_{PtH})$, of relative intensity 1:8:18:8:1 and the observed spectra are in accord with this prediction (see Figure 1 which also contains a diagram of the coupling scheme).

The $^{31}P\{^1H\}$ NMR spectra of **1** and **2** are also consistent with the presence of two equivalent Pt and four equivalent P atoms. The spectrum of **2** (Figure 2) again corresponds to the superposition of three subspectra arising from the three diplatinum combinations. In this case the nonactive Pt_2 isotopomer produces a single line at ν_P. Those molecules containing one ^{195}Pt nucleus constitute an $A_2A_2'X$ spin system and exhibit the requisite first-order spectrum, in contrast to similar binuclear species for which second-order spectra have been reported.[20,30,31] The resonance of the two phosphorus nuclei directly adjacent to the ^{195}Pt nucleus is split into a doublet by $^1J_{PtP}$ coupling and each doublet line is again split as a binomial triplet by coupling with the alternate magnetically nonequivalent phosphorus nuclei ($^3J_{PP}$). The resonance of these latter P atoms is affected in a similar manner, although the doublet separation is greatly decreased, $^2J_{PtP}$ vs. $^1J_{PtP}$. Thus from this subspectrum the values of $^1J_{PtP}$, $^2J_{PtP}$, and $^3J_{PP}$ are directly observable (Table II). The third binuclear isotopomer, $^{195}Pt_2$, corresponds to a closely coupled $A_2A_2'XX'$ system and does not give rise to a simple first-order spectrum. Rather, virtual coupling is observed.[20,30,31] This spin system has been thoroughly examined and the major feature of the spectrum is shown to be a doublet of separation N, where $N = (J_{AX} + J_{AX'})$ i.e., $({}^1J_{PtP} + {}^2J_{PtP})$ in this case.[32-34] The calculated and observed values for N are in excellent agreement (3107.5 vs. 3107.3 Hz and 3207.0 vs. 3207.0 Hz for **1** and **2**, respectively). That this N separation is greater than $^1J_{PtP}$ indicates that $^1J_{PtP}$ and $^2J_{PtP}$ are of similar sign and, as $^1J_{PtP} > 0$,[35] both are positive. Interestingly, $[Pt_2H_3(dppm)_2][PF_6]$ also exhibits positive values for these constants while in a number of closely associated binuclear complexes $^2J_{PtP}$ has been reported to be negative.[30] The theoretical intensity of each line of the N doublet is one-fourth of the entire A–A′ spectrum. Thus this is equivalent to ${}^1/_4$ on the relative scale which describes the populations of the three diplatinum isotopomers as 4:4:1 (Pt_2, ^{195}Pt–Pt, and $^{195}Pt_2$). This N line should therefore be equal in intensity to the flanking lines of adjacent $A_2A_2'X$ triplet ($4 \times {}^1/_4 \times {}^1/_4 = {}^1/_4$) as observed.

The remaining half of the $^{195}Pt_2$ spectrum is distributed in sets of doublet bands of varying intensity.[32] Figure 3 shows the low-field region in the spectrum of **2** and also contains a computer simulation of this portion of the $A_2A_2'XX'$ spectrum.[36] The bands designated $\chi_1(i)$, χ_2, and $\chi_1(o)$, along with the N doublet line, comprise the entire predicted low-field spectrum. The intensities and separations of these lines are functions of J_{AX}, $J_{AX'}$, $J_{AA'}$, and $J_{XX'}$, i.e., $^1J_{PtP}$, $^2J_{PtP}$, $^3J_{PP}$, and $^1J_{PtPt}$. It is directly possible to observe $^1J_{PtPt}$, as it corresponds to the separation between $\chi_1(i)$ and $\chi_1(o)$, and the values obtained are presented in Table II. As the other defining coupling constants are available from direct observation of the $A_2A_2'X$ spectrum discussed above, it is possible to check the observed $^1J_{PtPt}$ values by calculations involving the separations between the lines of the $\chi_1(i)$ doublet. This calculation for **2** yields a value of 840.7 Hz, in excellent agreement with that observed, 840.2 Hz. Similar calculations further substantiate these assignments; e.g., the separation between χ_2 doublets in the spectrum of **2** yields a value of 6.9 Hz for $^3J_{PP}$, which compares very well with the value of 6.8 Hz observed in the $A_2A_2'X$ spectrum.

The presence of terminal hydrido ligands, as indicated by the IR spectra of complexes **1**–**5**, is incompatible with the

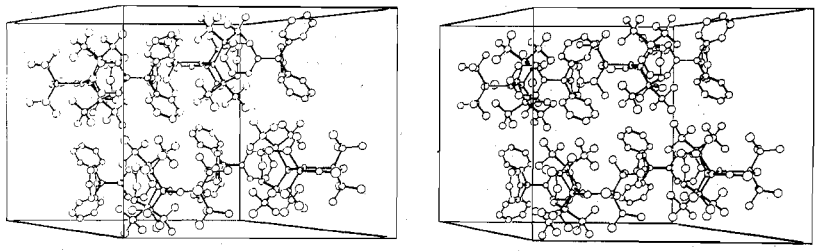

Figure 4. A stereoview of the unit cell of **2**, $[Pt_2H_3\{(t\text{-}Bu)_2P(CH_2)_3P(t\text{-}Bu)_2\}_2][BPh_4]$. Hydrogen atoms have been omitted for clarity. The x axis is vertical from top to bottom, the y axis is perpendicular to the paper going away from the reader, and the z axis is horizontal to the right. The vibrational ellipsoids are drawn at the 20% level here and in subsequent figures.

Scheme I

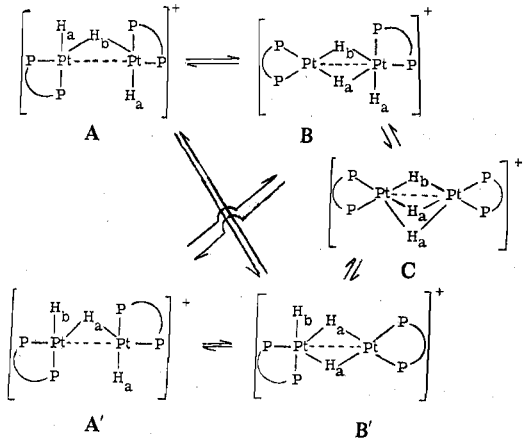

Scheme II

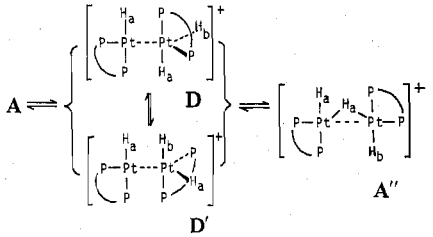

NMR results. The observed equivalence within the sets of H, P, and Pt nuclei may result from a facile hydrido ligand exchange between terminal and bridging sites, such as that represented in Scheme I. Both A and B are consistent with the IR data and a rapid interconversion of these two structures, possibly through the intermediacy of C, would explain the observed NMR features.

An alternative mechanism may involve a four- and five-coordinate Pt(II) pair (D) as a transient species formed by cleavage of the bridging H–Pt(II) bond (Scheme II). Regeneration of the bridged structure (A″) would account for the observed equivalence within the sets of H, P, and Pt nuclei. In the five-coordinate moiety a facile Berry pseudorotation[37] (D ⇄ D′) could be involved resulting in equilibration within the H and P sets (Scheme II). This appears to be more reasonable than the former process (Scheme I) which involves a six-coordinate d^8 moiety. The barriers to these rearrangements must be very low as no appreciable broadening of the hydride ^1H NMR signal is observed even at −108 °C in THF-d_8. The $^{31}P\{^1H\}$ NMR spectra of **1** and **2** are also temperature invariant. Minghetti et al.[21] have proposed a similar facile hydrido ligand exchange for $[Pt_2H_3(dppe)_2][BF_4]$ on the basis of its ^1H NMR spectrum, which is analogous to those of complexes **1–5**.

Description of the Structure of $[Pt_2H_3\{(t\text{-}Bu)_2P(CH_2)_3P(t\text{-}Bu)_2\}_2][B(C_6H_5)_4]$ (2). The crystal structure of **2** consists of the packing of four tetraphenylborate anions and four

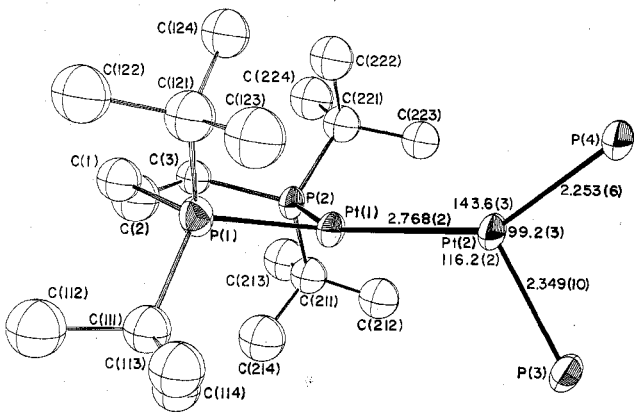

Figure 5. A perspective view of Pt(1) and its associated diphosphine ligand with Pt(2), P(3), and P(4) included. Hydrogen atoms have been omitted for clarity. The numbering scheme and selected distances and angles are also shown.

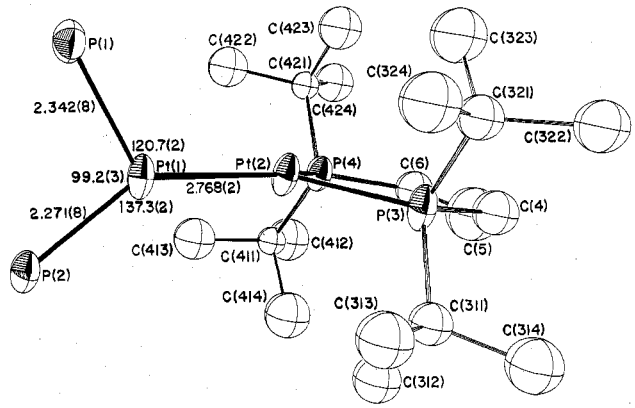

Figure 6. A perspective view of Pt(2) and its associated diphosphine ligand with Pt(1), P(1), and P(2) included. Hydrogen atoms have been omitted for clarity. The numbering scheme and selected distances and angles are also shown.

trihydridodiplatinum cations. A stereoscopic diagram of the unit cell is shown in Figure 4. Bond distances and angles are compiled in Tables VIII and IX. The ions are well separated as the closest intermolecular contact is calculated to be 2.39 Å between atoms H1C(2) and H1C(114). There are minimal contacts between cation and anion, the closest of which are 2.42 Å, HC(33)···H2C(414), and 2.47 Å, HC(25)···H2C(413). There are no anion–anion contacts below 3.0 Å. Note that these values are calculated from H atom positions derived by assuming a C–H distance at 0.95 Å. Figures 5 and 6 contain representations of the coordination spheres of the two Pt atoms and selected bond distances and angles for the Pt_2P_4 core. These figures also include the numbering scheme for the trihydridodiplatinum cation which will be used throughout this discussion. A stereoscopic view of the entire cation is shown in Figure 7.

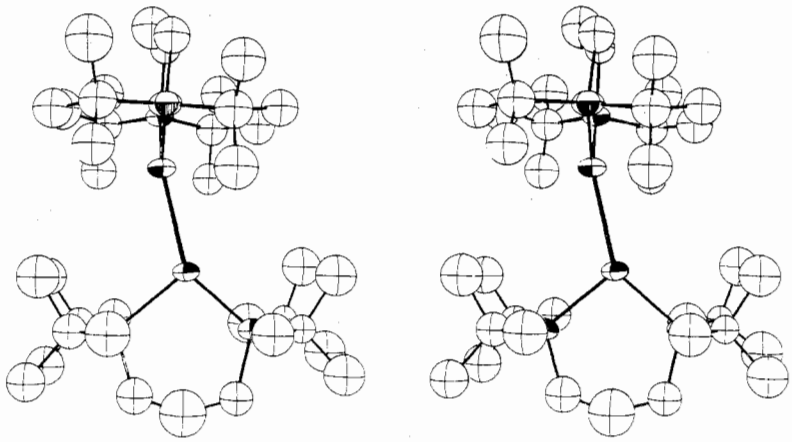

Figure 7. A stereoview of the entire cation, omitting hydrogen atoms. The chelate ring containing Pt(1) is perpendicular to the page.

Table VIII. Selected Distances (Å) in $[Pt_2H_3\{(t\text{-}Bu)_2P(CH_2)_3P(t\text{-}Bu)_2\}_2][B(C_6H_5)_4]$

Bond Distances

Pt(1)-Pt(2)	2.768 (2)	C(111)-C(112)	1.57 (5)
Pt(1)-P(1)	2.342 (8)	C(111)-C(113)	1.52 (5)
Pt(1)-P(2)	2.271 (8)	C(111)-C(114)	1.47 (4)
Pt(2)-P(3)	2.349 (10)	C(121)-C(122)	1.54 (5)
Pt(2)-P(4)	2.253 (6)	C(121)-C(123)	1.59 (6)
P(1)-C(1)	1.85 (4)	C(121)-C(124)	1.50 (5)
P(2)-C(3)	1.87 (4)	C(211)-C(212)	1.43 (7)
P(3)-C(4)	1.74 (4)	C(211)-C(213)	1.54 (5)
P(4)-C(6)	1.82 (4)	C(211)-C(214)	1.54 (5)
P(1)-C(111)	1.89 (3)	C(221)-C(222)	1.54 (5)
P(1)-C(121)	1.91 (3)	C(221)-C(223)	1.52 (6)
P(2)-C(211)	1.84 (4)	C(221)-C(224)	1.52 (6)
P(2)-C(221)	1.87 (3)	C(311)-C(312)	1.52 (4)
P(3)-C(311)	1.86 (3)	C(311)-C(313)	1.51 (4)
P(3)-C(321)	1.87 (3)	C(311)-C(314)	1.52 (7)
P(4)-C(411)	1.88 (3)	C(321)-C(322)	1.59 (6)
P(4)-C(421)	1.88 (3)	C(321)-C(323)	1.48 (4)
C(1)-C(2)	1.32 (4)	C(321)-C(324)	1.54 (4)
C(2)-C(3)	1.43 (4)	C(411)-C(412)	1.44 (4)
C(4)-C(5)	1.35 (4)	C(411)-C(413)	1.51 (7)
C(5)-C(6)	1.43 (6)	C(411)-C(414)	1.52 (5)
B-C(11)	1.65 (3)	C(421)-C(422)	1.55 (6)
B-C(21)	1.70 (4)	C(421)-C(423)	1.44 (4)
B-C(31)	1.68 (4)	C(421)-C(424)	1.50 (4)
B-C(41)	1.67 (5)		

Nonbonded Distances

Intermolecular

H1C(2)-H1C(114)	2.39		

Interligand

H1C(113)-H2C(324)	2.45	H3C(212)-H2C(312)	2.46

Intraligand

H2C(314)-H1C(4)	1.86	H1C(212)-H3C(214)	2.14
H3C(314)-H1C(322)	1.93	H2C(223)-H3C(413)	2.15
H3C(112)-H1C(7)	2.01	H1C(124)-H2C(1)	2.16
H1C(424)-H2C(6)	2.01	H3C(422)-H1C(413)	2.16
H2C(113)-H3C(123)	2.06	H1C(323)-H1C(4)	2.19
H3C(212)-H3C(223)	2.07	H2C(114)-H1C(2)	2.20
H3C(412)-H1C(6)	2.10	H2C(212)-H3C(213)	2.20
H2C(213)-H2C(3)	2.13		

The numbering scheme used for the tetraphenylborate anion is

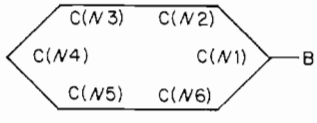

N = 1-4

The anion exhibits the usual distortions from ideal geometry.[38-40] The B–C bond lengths are equivalent and average 1.67 (5) Å (Table VIII), in good agreement with the average observed values of 1.66 (1) Å in $[Ni_2(OCN)_2(tren)_2][BPh_4]$,[39] where tren = triaminotriethylamine, and 1.67 (3) and 1.66 (3) Å in $[Ni(NH_2CH_2CH_2NH_2)_3][BPh_4]_2 \cdot 3(CH_3)_2SO$.[38] The C_{ipso}–B–C_{ipso} bond angles deviate from the tetrahedral value, ranging from 101 (2) to 115 (2)°, the pattern previously reported.[38] The boron atom is displaced an average of 0.11 Å from the planes of the phenyl rings in **2**. Similar distortions of 0.12, 0.12, and 0.11 Å have been cited by Cramer and Huneke[38] and Duggan and Hendrickson.[39]

Table IX. Selected Angles (deg) in $[Pt_2H_3\{(t\text{-}Bu)_2P(CH_2)_3P(t\text{-}Bu)_2\}_2][B(C_6H_5)_4]$

Pt(2)-Pt(1)-P(1)	120.7 (2)	C(4)-P(3)-C(311)	102 (2)
Pt(2)-Pt(1)-P(2)	137.3 (2)	C(4)-P(3)-C(321)	101 (2)
Pt(1)-Pt(2)-P(3)	116.2 (2)	C(311)-P(3)-C(321)	112 (1)
Pt(1)-Pt(2)-P(4)	143.6 (3)	C(6)-P(4)-C(411)	103 (1)
P(1)-Pt(1)-P(2)	99.2 (3)	C(6)-P(4)-C(421)	100 (1)
P(3)-Pt(2)-P(4)	99.2 (3)	C(411)-P(4)-C(421)	111 (1)
Pt(1)-P(1)-C(1)	113 (1)	C(1)-C(2)-C(3)	133 (3)
Pt(1)-P(2)-C(3)	116 (1)	C(4)-C(5)-C(6)	140 (4)
Pt(2)-P(3)-C(4)	113 (1)	P(1)-C(111)-C(112)	112 (3)
Pt(2)-P(4)-C(6)	118 (1)	P(1)-C(111)-C(113)	113 (2)
Pt(1)-P(1)-C(111)	112 (1)	P(1)-C(111)-C(114)	108 (2)
Pt(1)-P(1)-C(121)	111 (1)	P(1)-C(121)-C(122)	113 (2)
Pt(1)-P(2)-C(211)	112 (1)	P(1)-C(121)-C(123)	111 (3)
Pt(1)-P(2)-C(221)	110 (2)	P(1)-C(121)-C(124)	109 (2)
Pt(2)-P(3)-C(311)	113 (1)	P(2)-C(211)-C(212)	116 (2)
Pt(2)-P(3)-C(321)	114 (1)	P(2)-C(211)-C(213)	114 (3)
Pt(2)-P(4)-C(411)	112 (1)	P(2)-C(211)-C(214)	107 (2)
Pt(2)-P(4)-C(421)	111 (1)	P(2)-C(221)-C(222)	104 (2)
P(1)-C(1)-C(2)	119 (3)	P(2)-C(221)-C(223)	110 (3)
P(2)-C(3)-C(2)	117 (3)	P(2)-C(221)-C(224)	115 (2)
P(3)-C(4)-C(5)	126 (4)	P(3)-C(311)-C(312)	110 (2)
P(4)-C(6)-C(5)	119 (2)	P(3)-C(311)-C(313)	113 (2)
C(1)-P(1)-C(111)	103 (2)	P(3)-C(311)-C(314)	114 (2)
C(1)-P(1)-C(121)	101 (2)	P(3)-C(321)-C(322)	116 (2)
C(111)-P(1)-C(121)	115 (1)	P(3)-C(321)-C(323)	105 (2)
C(3)-P(2)-C(211)	106 (2)	P(3)-C(321)-C(324)	112 (2)
C(3)-P(2)-C(221)	104 (2)	P(4)-C(411)-C(412)	116 (2)
C(211)-P(2)-C(221)	108 (1)	P(4)-C(411)-C(413)	114 (2)
C(11)-B-C(21)	112 (2)	P(4)-C(411)-C(414)	110 (2)
C(11)-B-C(31)	112 (2)	P(4)-C(421)-C(422)	113 (2)
C(11)-B-C(41)	104 (2)	P(4)-C(421)-C(423)	109 (2)
C(21)-B-C(31)	101 (2)	P(4)-C(421)-C(424)	115 (2)
C(21)-B-C(41)	113 (2)		
C(31)-B-C(41)	115 (2)		

Tables VIII and IX contain a number of nonrepresentative distances and angles. For example, values of 133 (3) and 140 (3)° for angles C(1)–C(2)–C(3) and C(4)–C(5)–C(6) are clearly inappropriate for angles about saturated carbon atoms. Similarly the C(1)–C(2) bond length, 1.32 (4) Å, is unacceptably short for an sp^3–sp^3 carbon–carbon bond, which generally has a bond length of about 1.54 Å. The unusual

values associated with the hydrocarbon periphery of the diphosphine ligand presumably arise from the poor quality of the data.

The Pt(1)–Pt(2) separation in complex **2**, 2.768(2) Å, is equal to that found in $Pt_2[(t\text{-}Bu)_2P(CH_2)_3P(t\text{-}Bu)_2]_2$, 2.765 (1) Å.[17] This is noteworthy because, as pointed out by Churchill and co-workers,[41] all previously reported complexes containing unsupported μ_2-hydrido ligands have metal–metal separations significantly longer than those observed in analogous unbridged complexes. Recent tabulations of Pt–Pt bond separations[17,31,42,43] show that although a few complexes exhibit Pt–Pt bond lengths longer than 2.77 Å the majority have substantially shorter values. We have proposed[17] that the long Pt–Pt bond length in $Pt_2[(t\text{-}Bu)_2P(CH_2)_3P(t\text{-}Bu)_2]_2$ (**10**) may result from steric interactions between the hydrocarbon peripheries of the dimer halves. The bond elongation which would normally accrue from a μ_2-hydrido ligand is not observed in complex **2** because the unbridged complex itself has a distended Pt–Pt bond. We proposed that the ligand periphery is also largely responsible for the dihedral angle of 82° between coordination planes found in complex **10**. A similar value of 89° is observed in complex **2**. Figure 7 shows that as in $Pt_2[(t\text{-}Bu)_2P(CH_2)_3P(t\text{-}Bu)_2]_2$[17] methyl groups from one ligand fit into gaps in the hydrocarbon portion of the other diphosphine ligand.

The observed coordination sphere of each platinum center consists of another platinum and two phosphorus atoms in a highly distored trigonal array. The geminal P–Pt–P angles are identically 99.2 (3)°, equivalent to the analogous angle in $PtCl_2[(t\text{-}Bu)_2P(CH_2)_3P(t\text{-}Bu)_2]$, 99.1 (2)°.[44] In $Pt_2[(t\text{-}Bu)_2P(CH_2)_3P(t\text{-}Bu)_2]_2$, this angle is 102.4 (2)°.[17] The smaller values found in the Pt(II) complexes may arise from a decrease in π bonding because the metal is in the higher oxidation state as suggested previously.[17,45] Note that this angle retains a value of approximately 99° in the Pt(II) complexes despite major differences in the local environments. Presumably this value represents a lower limit which is imposed on the chelating angle by the bulk of the *tert*-butyl groups bound to the phosphorus atoms. Table VIII lists a number of close H···H intraligand contacts which would become more severe upon additional contraction of the P–Pt–P angle.

In each Pt(diphos) moiety of **2** one Pt–P distance is longer than the other: 2.342 (8) Å (Pt(1)–P(1)) vs. 2.271 (8) Å (Pt(1)–P(2)) and 2.349 (10) Å (Pt(2)–P(3)) vs. 2.253 (6) Å (Pt(2)–P(4)). Compare these distances with the average distance of 2.28 Å found in $PtCl_2[(t\text{-}Bu)_2P(CH_2)_3P(t\text{-}Bu)_2]$.[44] The Pt–Pt vector of **2** does not bisect the P–Pt–P angle. The Pt–Pt–P angles involving the shorter Pt–P bonds are larger than those of the longer bonds: 137.3 (2)° (Pt(2)–Pt(1)–P(2)) vs. 120.7 (2)° (Pt(2)–Pt(1)–P(1)) and 143.6 (3)° (Pt(1)–Pt(2)–P(4)) vs. 116.2 (2)° (Pt(1)–Pt(2)–P(3)). For comparison, the approximately D_{2d} structure of $Pt_2[(t\text{-}Bu)_2P(CH_2)_3P(t\text{-}Bu)_2]_2$[17] exhibits similar Pt–Pt–P angles of 128.5°. The Pt(2) atom in **2** is displaced 0.23 Å from the Pt(1)-P(1)P(2) plane while the Pt(1) atom is displaced 0.14 Å from the plane defined by Pt(2)P(3)P(4). The planes Pt(1)P(1)P(2) and Pt(2)P(3)P(4) form angles of 4.8 and 2.9°, respectively, with the Pt–Pt vector.

MO calculations on ML_5 systems indicate that for metal centers of d^8 configuration trigonal-bipyramidal (tbp) rather than square-pyramidal (sp) structures are favored.[46] The calculations have also shown that the axial σ bonds in tbp d^8 complexes are stronger than the apical bonds.[47] On the basis of these MO calculations the observed geometrical features of **2** may be rationalized in terms of interlocking distorted tbp structures which result in a structure analogous to A, containing one bridging and two terminal hydrido ligands. The positions of the missing terminal and bridging hydrido ligands can thus be assigned in terms of vacant tbp ligand sites. The P(2) and P(4) atoms occupy axial positions and the P(1) and P(3) atoms equatorial sites since the Pt(1)–P(2) and Pt(2)–P(4) distances are shorter than the Pt(1)–P(1) and Pt(2)–P(3) distances, respectively. The tbp structure shown as E_1 for the Pt(1) coordination sphere requires that the planes

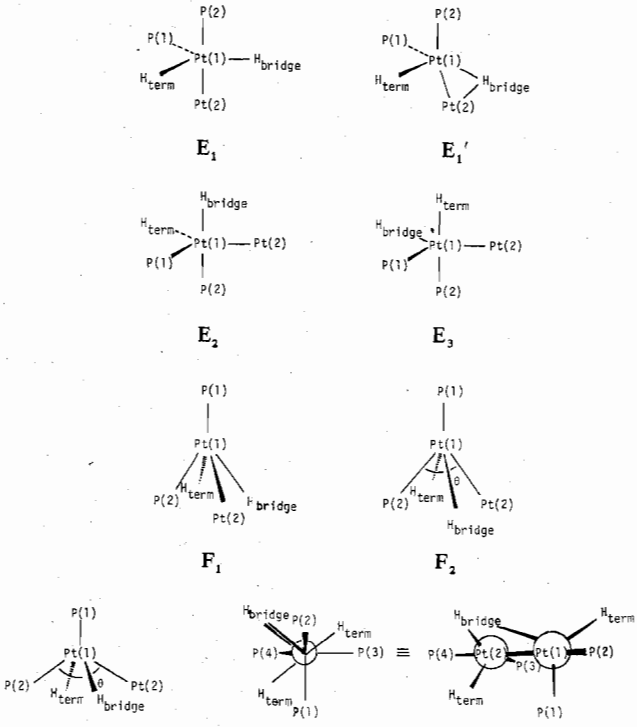

Pt(1)P(1)P(2) and Pt(2)P(3)P(4) each be coplanar with the Pt–Pt vector. This criterion is nearly met by the observed structure of **2**. Alternative alignments such as Pt(2)eq–Pt-(1)–P(1)eq (E_2 or E_3) are readily excluded because of the large discrepancy between the observed (2.9–4.8°) and the expected (120°) deviations from coplanarity. Also, the larger Pt(2)–Pt(1)–P(2) and Pt(1)–Pt(2)–P(4) angles, as compared with those of Pt(2)–Pt(1)–P(1) and Pt(1)–Pt(2)–P(3), are consistent with structure E_1. Thus the sole rational disposition for each tbp structure is analogous to E_1'. In the alternative sp geometry two ligand arrangements, shown as F_1 and F_2 for the Pt(1) fragment, are possible. Structure F_1 is excluded because of the large predicted angle between the Pt–Pt vector and the P(1)Pt(1)P(2) and P(3)Pt(2)P(4) planes. Structure F_2 conforms roughly to the observed geometry of the Pt(2)Pt(1)P(2) moiety only when the Pt(2)–Pt(1)–P(2) angle, θ, is considerably enlarged as in F_2'. Such a flattened sp structure becomes almost equivalent to the distorted tbp E_1. Thus the geometrical alignments around the Pt atoms are best described as highly distorted tbp with axial Pt(2) and P(2) and equatorial P(1) atoms about Pt(1) and axial Pt(1) and P(4) and equatorial P(3) atoms about Pt(2). The bridging hydrido ligand position can then be assigned by using the assumption that the bridging hydride is situated equidistant from the Pt atoms and lies in a plane bisecting the dihedral angle between the planes Pt(1)P(2)P(3) and Pt(2)P(3)P(4). The proposed overall structure is shown as G. The terminal hydrido ligands are accommodated at the vacant equatorial positions.

Discussion

In our investigations of the chemistry of a series of novel *cis*-(diphosphine)dihydridoplatinum and related bis(diphosphine)diplatinum complexes, we have isolated new bi-

nuclear complexes of the form $[Pt_2H_3(diphos)_2]X$ (X = Cl, OMe, BPh_4). While our work was in progress two reports concerning the preparation of similar complexes appeared.[20,21] An entirely analogous trihydridodiplatinum cation was produced by the action of methanolic KBH_4 on $[Pt(PzH)_2(dppe)]^{2+}$,[21] where PzH represents the excellent leaving group 3,5-dimethylpyrazole.[21] Similar treatment of $PtCl_2(dppm)$ yielded $[Pt_2H_3(dppm)_2]Cl$, which could also be prepared from the Pt(I) dimer $Pt_2Cl_2(dppm)_2$.[20] The dppm ligands in both of these binuclear complexes have been shown to bridge, rather than chelate, the Pt atoms.[20,30] This behavior probably results from relief of the unfavorable ring strain inherent in the four-membered chelate ring, which is relieved by formation of a five-membered bridging ring. Brown et al.[20] have suggested that the stability of the $Pt_2H_3P_4$ core is a result of the bridged $Pt_2(dppm)_2$ skeleton. The isolation of complexes **1–5** and $[Pt_2H_3(dppe)_2][BF_4]$[21] from a variety of synthetic pathways clearly refutes this proposal.

We have found three methods to prepare $[Pt_2H_3(diphos)_2]^+$ cations. When considered in conjunction with the alcoholic tetrahydidoborate method these apparently unrelated synthetic pathways suggest a common key step involving a *cis*-dihydride complex. As outlined above the facile formation of **1** from the reaction of *cis*-$PtH_2[(t\text{-}Bu)_2P(CH_2)_2P(t\text{-}Bu)_2]$ with $PtClH[(t\text{-}Bu)_2P(CH_2)_2P(t\text{-}Bu)_2]$ implies that the chloroform reaction proceeds through the interaction of a *cis*-dihydride with a hydridochloro intermediate. Complex **3** is formed in a similar reaction of $PtH_2[(t\text{-}Bu)_2P(CH_2)_3P(t\text{-}Bu)_2]$ with its hydridomethoxy analogue, both of which are produced in the course of oxidative addition of methanol to $Pt_2[(t\text{-}Bu)_2P(CH_2)_3P(t\text{-}Bu)_2]_2$ (eq 3 and 4). By analogy, a probable intermediate in the formation of the $[Pt_2H_3(dppe)_2]^+$ cation is the mononuclear *cis*-dihydride complex $PtH_2(dppe)$, which could readily form by the reaction at BH_4^- with $[Pt(PzH)_2(dppe)]^{2+}$.[21] In fact we obtained evidence for this *cis*-dihydride complex from the Na/Hg reduction of $PtCl_2(dppe)$ under H_2 atmosphere.[17] In this case the *cis*-dihydride complex could react with $[PtH(PzH)(dppe)]^+$ or $[PtH(MeOH)(dppe)]^+$, also formed by treatment of $[Pt(PzH)_2(dppe)]^{2+}$ with methanolic BH_4^-. Thus the pivotal step in binuclear cation formation may be

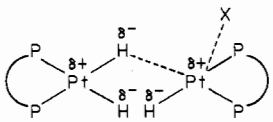

where X is Cl^-, MeO^-, PzH, or MeOH. The partial anionic character of the hydrido ligands results from the trans influence of the cis phosphorus atoms.[48] This step can thus be viewed as a nucleophilic substitution of X in PtHX(diphos) by the incoming hydrido ligand. In the formation of the cationic dppm complex from $PtCl_2(dppm)$ a similar step may take place following which diphosphine rearrangement occurs.

In contrast to the *cis*-dihydride complexes, *trans*-dihydrides PtH_2L_2 (L = P(*i*-Pr)$_3$ (*i*-Pr = isopropyl), $PPh(t\text{-}Bu)_2$) react with $CHCl_3$ to give *trans*-$PtClHL_2$ exclusively, no cationic trihydride complexes being formed.[12] This is surprising as a hydrido ligand should exert a stronger trans influence than a phosphine,[49] thereby increasing the nucleophilicity of the trans hydrido ligand. The cone angles[50] of P(*i*-Pr)$_3$ and $PPh(t\text{-}Bu)_2$, 160 ± 10 and 170 ± 2°,[51] respectively, are larger than the calculated value of 150° for each P atom of $(t\text{-}Bu)_2P(CH_2)_2P(t\text{-}Bu)_2$,[17] and the bulk of the monodentate phosphines may prevent the nucleophilic attack of a hydrido ligand of the *trans*-dihydride complex on the $PtClHL_2$ species. An alternative explanation involves a relative increase in the reactivity of *trans*-PtH_2L_2 toward $CHCl_3$ vs. that toward *trans*-$PtClHL_2$. Thus the rate constant k_1 of the chloroform reaction may be larger than k_2 for the *trans*-dihydride complexes while the reverse may be true for the *cis*-dihydride complex, i.e., $k_1' < k_2'$.

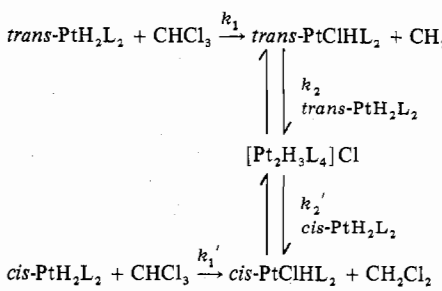

Another interesting difference in reactivity is observed in *cis*-dihydride complexes with varying diphosphine ligands. Chloroform produces not only a trihydrido binuclear cation upon reaction with $PtH_2[(t\text{-}Bu)_2P(CH_2)_2P(t\text{-}Bu)_2]$ but also $PtCl_2[(t\text{-}Bu)_2P(CH_2)_2P(t\text{-}Bu)_2]$. No *cis*-diphosphine dichloride complex is produced if the diphosphine is $(t\text{-}Bu)_2P(CH_2)_3P(t\text{-}Bu)_2$, implying a decrease in Pt–H reactivity. Supporting this is the fact that the seven-membered chelate diphosphine complex *cis*-$PtH_2[(t\text{-}Bu)_2PCH_2C_6H_4CH_2P(t\text{-}Bu)_2]$ is stable enough in $CHCl_3$ to permit NMR study.[16] This decrease in Pt–H reactivity with increasing chelate ring size parallels the increase in ν_{PtH} with increasing ring size.[17] These trends are explicable in terms of the trans influence of the diphosphine ligand which will be at a maximum for PPtP angles near 90°. These chelate angles for $(t\text{-}Bu)_2P(CH_2)_2P(t\text{-}Bu)_2$ and $(t\text{-}Bu)_2P(CH_2)_3P(t\text{-}Bu)_2$ in the *cis*-$PtCl_2$(diphos) complexes are 89.4 (1)°[52] and 99.1 (1)°,[44] respectively. Thus the five-membered chelate ring exerts a more efficient trans influence. Additionally, the reactivity of the *cis*-dihydride complexes may be kinetically influenced by differing steric requirements. An increase in chelate ring size should lead to an increase in the steric crowding around the PtH_2 moiety by the *tert*-butyl groups and thereby prevent approach of $CHCl_3$.

A decrease in the value of $\nu_{Pt-H(terminal)}$ is observed in the cationic trihydridodiplatinum complexes on going from a six- to a five-membered chelate ring. This may result from a more efficient diphosphine trans influence in **1**, as proposed above. Substitution of *tert*-butyl groups by phenyl groups should reduce the trans influence by lowering the basicity of the P atoms. Consistently, the value of $\nu_{Pt-H(terminal)}$ is higher for **4** (2010 cm^{-1}) than for **1** (2000 cm^{-1}). However, upon further phenyl substitution the trend reverses, $[Pt_2H_3(dppe)_2][BF_4]$ showing $\nu_{Pt-H(terminal)}$ at 2000 cm^{-1}.[21] Identical behavior has been noted for the mononuclear *cis*-dihydride complexes in which ν_{Pt-H} for $PtH_2[Ph(t\text{-}Bu)P(CH_2)_2PPh(t\text{-}Bu)]$ is higher than that for either *tert*-butyl or phenyl complexes.[17]

The value of $^1J_{PtH}$ also varies with chelate ring size and diphosphine substitution. In the *cis*-dihydride complexes we found that ring size affects the hybridization of the metal center: the smaller the ring size the larger the s character of the bonding orbitals of the platinum atoms.[17] This effect is also observed in the $^1J_{PtH}$ values of $[Pt_2H_3\{(t\text{-}Bu)_2P(CH_2)_nP(t\text{-}Bu)_2\}_2]^+$ complexes, n = 2 or 3. Unlike the case for $\nu_{Pt-H(terminal)}$ this coupling constant shows a monotonic increase on substitution of Ph for *t*-Bu, with values of 443, 467, and 500 Hz for $(t\text{-}Bu)_2P(CH_2)_2(t\text{-}Bu)_2$, $Ph(t\text{-}Bu)P(CH_2)_2PPh(t\text{-}Bu)_2$, and $Ph_2P(CH_2)_2PPh_2$,[21] respectively. The small values of $^1J_{PtH}$, 395–500 Hz, for the cationic trihydridodiplatinum complexes, which may be compared with values of 1050–1140 Hz in the *cis*-dihydride complexes,[16,17] are consistent with their fluxional behavior. The former values are among the lowest reported; cf. $^1J_{PtH}$ = ca. 790 Hz in *trans*-PtH_2L_2 [L = P(*i*-Pr)$_3$, PCy_3, $PPh(t\text{-}Bu)_2$].[12] Similar small values for bridging hydrido ligands have been reported

for $Pt_2(\mu\text{-}H)_2[Si(OEt)_3]_2[PMe(t\text{-}Bu)_2]_2$ (456 Hz)[19] and $[Pt_2H_3(dppm)_2][PF_6]$ (540 Hz).[20]

The parameters derived from the $^{31}P\{^1H\}$ NMR spectra of **1** and **2** are useful. As pointed out by Boag et al.[31] $^1J_{PtPt}$ values vary widely and show no apparent correlation with internuclear separation. Thus it is difficult to assess the significance of these couplings observed in **1** and **2** (Table II) other than to recognize that they undoubtedly result from a direct Pt–Pt bond, as suggested by the solid-state structure, and not merely from transfer of spin information through a bridging hydrido ligand. This is substantiated by the nonzero $^3J_{PP}$ coupling constant. For comparison, the complex $Pt_2(\mu\text{-}H)_2[Si(OEt)_3]_2[PMe(t\text{-}Bu)_2]_2$ has $^1J_{PtPt}$, $^1J_{PtP}$, $^2J_{PtP}$, and $^3J_{PP}$ values of 92, +3125, +68, and 0 Hz.[19,31] This complex is thought to have a Pt–Pt distance of approximately 2.69 Å by analogy with the structurally characterized complex $Pt_2(\mu\text{-}H)_2(SiEt_3)_2(PCy_3)_2$.[19] The values of these constants in **2**, 840.2, +3039.0, +168.0, and 6.8 Hz, can also be compared with those found in $Pt_2[(t\text{-}Bu)_2P(CH_2)_3P(t\text{-}Bu)_2]_2$,[17] $^1J_{PtP}$ = 3945, $^2J_{PtP}$ = 178.3, and $^3J_{PP}$ = 32.6 Hz. As expected, all of these observed constants are consistent with weakened bonding in all facets of the Pt_2P_4 core. The direct Pt–Pt coupling constant was not derived for the Pt(0) dimer, as the spectral quality was poor and no fine structure was observed. In the absence of high-resolution data we had interpreted the $^{195}Pt_2$ subspectrum in purely first-order terms.[17] In retrospect this assignment must be wrong and the true nature of the spin system must be analogous to that observed for complexes **1** and **2**.

Finally, the apparent equivalence within the sets of hydrido and phosphorus ligands for the $[Pt_2H_3(diphos)_2]^+$ complexes in solution, as judged by their ^1H and ^{31}P NMR spectra, deserves comment. The observed solid-state structure of complex **2** indicates inequivalence of the two phosphorus atoms attached to each Pt center and the IR spectra are consistent with the presence of both bridging and terminal hydrido ligands. For the proposed structure, A or G, which involves two interlocking tbp fragments, the most probable mechanism for exchange is represented in Scheme II. The distortions from ideal tbp geometries in complex **2** are large and severe strain must be present, especially with regard to the acute Pt(2)–Pt(1)–H_{bridge} and Pt(1)–Pt(2)–H_{bridge} angles. This strain could be a factor in lowering the energy barrier for cleavage of the hydride bridge bond which would result in a facile transformation to species D. The five-coordinate moiety of D should be subject to a ready Berry pseudorotation which, for d^8 tbp complexes, is a symmetry-allowed process characterized by low barriers.[53,54] The hydrido and phosphorus ligands would be exchanged by such a process. Re-formation of the hydride bridge bonding and subsequent exchange at the alternate Pt center would result in the equivalence observed within the H, P, and Pt sets. The bridge terminal hydrido ligand exchange in $[Pt_2H_3(dppm)_2][PF_6]$[20] is slow compared with those of complexes **1**–**5** and $[Pt_2H_3(dppe)_2][BF_4]$,[21] occurring only above 70 °C. Steric constraint arising from the bridging dppm ligands and the Pt–Pt bond may inhibit a facile Berry pseudorotation and thereby give rise to the high activation energy for equilibration of the hydrido ligand.[55] These fluxional processes are of obvious interest and merit further investigation.

Acknowledgment. This work was supported by National Science Foundation (Grant CHE 76-10335) and the Japanese Society for the Promotion of Science under the Japan–U.S. Cooperative Science Program (Grant GR021/INT 77-07152).

Registry No. **1**, 70084-51-4; **2**, 70072-47-8; **3**, 70095-71-5; **4**, 70072-49-0; **5**, 70072-50-3; **6**, 70072-51-4; **7**, 66467-69-4; **8**, 66467-71-8; **9**, 66467-55-8; **10**, 66467-51-4; $PtCl_2[(t\text{-}Bu)_2P(CH_2)_2P(t\text{-}Bu)_2]$, 61829-17-2; $Pt_2[Ph(t\text{-}Bu)P(CH_2)_2PPh(t\text{-}Bu)]_2$, 70084-49-0.

Supplementary Material Available: Tables VI and VII (idealized hydrogen atom positions and root-mean-square amplitudes of vibration) and a listing of the observed and calculated structure amplitudes (27 pages). Ordering information is given on any current masthead page.

References and Notes

(1) (a) Northwestern University. (b) Osaka University.
(2) Hieber, W.; Leutert, F. *Naturwissenschaften* **1931**, *19*, 360.
(3) Muetterties, E. L., Ed. "Transition Metal Hydrides"; Marcel Dekker: New York, 1971.
(4) Kaesz, H. D.; Saillant, R. B. *Chem. Rev.* **1972**, *72*, 231.
(5) Cooper, C. B., III; Shriver, D. F.; Onaka, S. *Adv. Chem. Ser.* **1978**, *No. 167*, 232.
(6) (a) Frenz, B. A.; Ibers, J. A. In "Transition Metal Hydrides"; Muetterties, E. L., Ed.; Marcel Dekker: New York, 1971; p 33. (b) Ibers, J. A. *Adv. Chem. Ser.* **1978**, *No. 167*, 26. (c) Bau, R.; Teller, R. G.; Kirtley, S. W.; Koetzle, T. F. *Acc. Chem. Res.* **1979**, *12*, 176.
(7) Tolman, C. A. In "Transition Metal Hydrides"; Muetterties, E. L., Ed.; Marcel Dekker: New York, 1971; p 271.
(8) Chatt, J.; Duncanson, L. A.; Shaw, B. L. *Proc. Chem. Soc., London* **1957**, 343.
(9) Hartley, F. R. "The Chemistry of Platinum and Palladium"; Applied Science: London, 1973.
(10) Belluco, U. "Organometallic and Coordination Chemistry of Platinum"; Academic Press: New York, 1974.
(11) Gerlach, D. H.; Kane, A. R.; Parshall, G. W.; Jesson, J. P.; Muetterties, E. L. *J. Am. Chem. Soc.* **1971**, *93*, 3543.
(12) Yoshida, T.; Otsuka, S. *J. Am. Chem. Soc.* **1977**, *99*, 2134.
(13) Shaw, B. L.; Uttley, M. F. *J. Chem. Soc., Chem. Commun.* **1974**, 918.
(14) Green, M.; Howard, J. A. K.; Spencer, J. L.; Stone, F. G. A. *J. Chem. Soc., Chem. Commun.* **1975**, 3.
(15) Immirzi, A.; Musco, A.; Carturan, G.; Belluco, U. *Inorg. Chim. Acta* **1975**, *12*, L23.
(16) Moulton, C. J.; Shaw, B. L. *J. Chem. Soc., Chem. Commun.* **1976**, 365.
(17) Yoshida, T.; Yamagata, T.; Tulip, T. H.; Ibers, J. A.; Otsuka, S. *J. Am. Chem. Soc.* **1978**, *100*, 2063.
(18) Green, M.; Howard, J. A. K.; Proud, J.; Spencer, J. L.; Stone, F. G. A.; Tsipis, C. A. *J. Chem. Soc., Chem. Commun.* **1976**, 671.
(19) Ciriano, M.; Green, M.; Howard, J. A. K.; Proud, J.; Spencer, J. L.; Stone, F. G. A.; Tsipis, C. A. *J. Chem. Soc., Dalton Trans.* **1978**, 801.
(20) Brown, M. P.; Puddephatt, R. J.; Rashidi, M.; Seddon, K. R. *J. Chem. Soc., Dalton Trans.* **1978**, 516; *Inorg. Chim. Acta* **1977**, *23*, L27.
(21) Minghetti, G.; Banditelli, G.; Bandini, A. L. *J. Organomet. Chem.* **1977**, *139*, C80.
(22) Corfield, P. W. R.; Doedens, R. J.; Ibers, J. A. *Inorg. Chem.*, **1967**, *6*, 197.
(23) Doedens, R. J.; Ibers, J. A. *Inorg. Chem.* **1967**, *6*, 204.
(24) The Northwestern absorption program, AGNOST, includes the Coppens–Leiserowitz–Rabinovitch logic for Gaussian integration and the Tompa analytical method. In addition to various local programs for the CDC 6600 computer, modified versions of the following programs were employed: Zalkin's FORDAP Fourier summation program, Johnson's ORTEP thermal ellipsoid plotting program, and Busing and Levy's ORFFE error function program. Our full-matrix, least-squares program, NUCLS, in its nongroup form closely resembles the Busing–Levy ORFLS program. Final calculations were performed by remote telephone hookup to the CDC 7600 computer at Lawrence Berkeley Laboratory. The same programs were used. The diffractometer was run under the disk-oriented Vanderbilt system: Lenhert, P. G. *J. Appl. Crystallogr.* **1975**, *8*, 568.
(25) Cromer, D. T.; Waber, J. T. "International Tables for X-Ray Crystallography"; Kynoch Press: Birmingham, England, 1974; Vol. IV, Tables 2.2A.
(26) Stewart, R. F.; Davidson, E. R.; Simpson, W. T. *J. Chem. Phys.* **1965**, *42*, 3175.
(27) Cromer, D. T.; Liberman, D. *J. Chem. Phys.* **1970**, *53*, 1891.
(28) La Placa, S. J.; Ibers, J. A. *Acta Crystallogr.* **1965**, *18*, 511.
(29) Supplementary material.
(30) Brown, M. P.; Puddephatt, R. J.; Rashidi, M.; Seddon, K. R. *J. Chem. Soc., Dalton Trans.* **1977**, 951.
(31) Boag, N. M.; Browning, J.; Crocker, C.; Goggin, P. L.; Goodfellow, R. J.; Murray, M.; Spencer, J. L. *J. Chem. Res.* (*S*) **1978**, 228; *J. Chem. Res.* (*M*) **1978**, 2962.
(32) Harris, R. K.; Woplin, J. R.; Dunmur, R. E.; Murray, M.; Schmutzler, R. *Ber. Bunsenges. Phys. Chem.* **1972**, *76*, 44.
(33) Harris, R. K.; Woodman, C. M. *Mol. Phys.*, **1966**, 437.
(34) Harris, R. K. *Can. J. Chem.*, **1964**, *42*, 2275.
(35) McFarlane, W. *J. Chem. Soc. A* **1967**, 1922.
(36) The six-spin system was simulated by using the program NMRPLOT obtained from Professor J. Lambert of Northwestern University and modified by Dr. D. L. Thorn.
(37) Berry, R. S. *J. Chem. Phys.* **1960**, *32*, 733.
(38) Cramer, R. E.; Huneke, J. T. *Inorg. Chem.* **1978**, *17*, 365.
(39) Duggan, D. M.; Hendrickson, D. N. *Inorg. Chem.*, **1974**, *13*, 2056.
(40) DiVaira, M.; Orlandini, A. B. *J. Chem. Soc., Dalton Trans.* **1972**, 1704.
(41) (a) Churchill, M. R.; DeBoer, B. G.; Rotella, F. J. *Inorg. Chem.* **1976**, *15*, 1843. (b) Churchill, M. R.; Julis, S. A.; Rotella, F. J. *Ibid.* **1977**, *16*, 1137.
(42) Green, M.; Howard, J. A. K.; Laguna, A.; Smart, L. E.; Spencer, J. L.; Stone, F. G. A. *J. Chem. Soc., Dalton Trans.* **1977**, 278.

(43) Wagner, K. P.; Hess, R. W.; Treichel, P. M.; Calabrese, J. C. *Inorg. Chem.* **1975**, *14*, 1121.
(44) Kasai, N., private communication.
(45) Nakamura, A.; Yoshida, T.; Cowie, M.; Otsuka, S.; Ibers, J. A. *J. Am. Chem. Soc.* **1977**, *99*, 2108.
(46) Elian, M.; Hoffmann, R. *Inorg. Chem.* **1975**, *14*, 1058.
(47) Rossi, A. R.; Hoffmann, R. *Inorg. Chem.* **1975**, *14*, 365.
(48) Huheey, J. E. In "Inorganic Chemistry"; Harper and Row: New York, 1972; p 227.
(49) Appleton, T. G.; Clark, H. C.; Manzer, L. E. *Coord. Chem. Rev.* **1973**, *10*, 335.
(50) Tolman, C. A. *J. Am. Chem. Soc.* **1970**, *92*, 2956.
(51) Otsuka, S.; Yoshida, T.; Matsumoto, M.; Nakatsu, K. *J. Am. Chem. Soc.* **1976**, *98*, 5850.
(52) Harada, M.; Kai, Y.; Yasuoka, N.; Kasai, N. *Bull. Chem. Soc. Jpn.*, **1976**, *49*, 3472.
(53) Pearson, R. G. "Symmetry Rules for Chemical Reactions"; Wiley-Interscience: New York, 1976; p 190.
(54) Eaton, D. R.; *J. Am. Chem. Soc.* **1968**, *90*, 4272.
(55) The preparation and structural characterization of another Pt complex containing both bridging and terminal hydrido ligands, $[Pt_2H_2Ph(PEt_3)_4][BPh_4]$ (Bracher, G.; Grove, D. M.; Venanzi, L. M.; Bachechi, F.; Mura, P.; Zambonelli, L. *Angew. Chem., Int. Ed. Engl.* **1978**, *17*, 778), has recently appeared. No indication of bridge–terminal hydrido ligand exchange is observed at room temperature. This lack of fluxionality is presumably also a result of steric constraint. The PEt_3 ligands of each Pt center are mutually trans and would not be readily accommodated in the tbp geometry outlined above. The complex is best described as two distorted square-planar d^8 moieties sharing the bridging hydrido ligand and involving a minimal Pt–Pt interaction. Thus the complex lacks the angular strain present in complexes **1–5** which facilitates bridge bond cleavage.

Contribution from the Departments of Inorganic Chemistry, University of Manchester, Manchester M13 9PL, England, and University of Newcastle upon Tyne, Ne1 7RU, England

Preparation and Characterization of Tetraphenylarsonium *trans*-Bis(μ-acetato)-tetrachlorodimolybdate(II) Disolvates, $[(C_6H_5)_4As]_2[Mo_2(O_2CCH_3)_2Cl_4]\cdot 2L$ (L = H_2O or CH_3OH)

WILLIAM CLEGG,*[1a] C. DAVID GARNER,*[1b] STEPHEN PARKES,[1b] and IAN B. WALTON[1b]

Received December 15, 1978

The preparation and isolation of $[(C_6H_5)_4As]_2[Mo_2(O_2CCH_3)_2Cl_4]\cdot 2L$ (L = H_2O or CH_3OH) are reported. The methanolate crystallizes in the triclinic space group $P\bar{1}$ with a = 10.571 (2) Å, b = 11.330 (2), Å, c = 13.397 (2) Å, α = 75.16 (1)°, β = 67.19 (1)°, and γ = 64.24 (1)°. The structure has been determined from 2165 X-ray counter intensities by Patterson and Fourier techniques and refined by full-matrix least-squares methods to R = 0.058 (0.073 weighted). The unit cell contains one centrosymmetric $[Mo_2(O_2CCH_3)_2Cl_4]^{2-}$, two $[(C_6H_5)_4As]^+$ ions, and two CH_3OH moieties. The anion has the trans configuration and closely approximates to D_{2h} point symmetry with dimensions Mo–Mo = 2.086 (2), $\overline{\text{Mo–O}}$ = 2.120 (13), and $\overline{\text{Mo–Cl}}$ = 2.434 (4) Å; the methanol molecules are not coordinated to the molybdenum atoms. Vibrational and electronic spectral data are reported for this material. The ν(Mo–Mo) stretching frequency of 380 cm^{-1} and the position of the first absorption maximum at 20 200 cm^{-1} are midway between the corresponding values of $Mo_2(O_2CCH_3)_4$ and $[Mo_2Cl_8]^{4-}$, even though the Mo–Mo bond length for $[Mo_2(O_2CCH_3)_2Cl_4]^{2-}$ is the shortest of these three complexes.

Introduction

A large number of compounds containing metal–metal quadruple bonds have now been characterized,[2,3] including a considerable range of compounds containing the Mo_2^{4+} center. Two parent complexes, from which a large number of these derivatives have been prepared, are $Mo_2(O_2CCH_3)_4$[4] and $[Mo_2Cl_8]^{4-}$.[5] Herein[6] we report the isolation, X-ray crystallographic characterization, and certain spectroscopic properties of the bis(μ-acetato)-tetrachlorodimolybdenum(II) complex, *trans*-$[Mo_2(O_2CCH_3)_2Cl_4]^{2-}$. Spectral properties of this anion are discussed with reference to the corresponding properties of $Mo_2(O_2CCH_3)_4$ and $[Mo_2Cl_8]^{4-}$.

Experimental Section

Preparation of $[(C_6H_5)_4As]_2[Mo_2(O_2CCH_3)_2Cl_4]\cdot 2L$ (L = H_2O or CH_3OH). $Mo_2(O_2CCH_3)_4$[4] (1.0 g, 2.34 mmol) was added to a solution of Ph_4AsCl (Aldrich, 1.92 g, 4.68 mmol) in deionized, degassed water (65 cm^3) under an atmosphere of purified nitrogen. Concentrated hydrochloric acid (20 cm^3), previously purged with nitrogen, was added dropwise with stirring to this solution. After ca. 8 h the orange precipitate which had formed was removed by filtration, washed twice with degassed, deionized water (10 cm^3) and methanol (2 × 5 cm^3), and dried in vacuo. Yield of $[(C_6H_5)_4As]_2[Mo_2(O_2CCH_3)_2Cl_4]\cdot 2H_2O$ was typically ca. 2 g (ca. 75%). Anal. Calcd for $C_{52}H_{50}O_6As_2Cl_4Mo_2$: C, 49.8; H, 4.0; As, 11.9; Cl, 11.3; Mo, 15.3. Found: C, 49.7; H, 3.9; As, 11.2; Cl, 11.7; Mo, 15.4. Crystals of $[(C_6H_5)_4As]_2[Mo_2(O_2CCH_3)_2Cl_4]\cdot 2CH_3OH$ suitable for X-ray crystallographic studies were obtained by recrystallization from degassed AnalaR methanol.

Data Collection and Reduction. The dark red crystals were irregular in shape. Initial values of the triclinic cell parameters were obtained from precession photographs (Mo Kα radiation, 0.710 69 Å) by a least-squares refinement based on the observed and calculated positions of spots on ($0kl$), ($h0l$), and ($hk0$) photographs. There were no systematic absences.

The crystal chosen for refinement of cell parameters and collection of intensities had a maximum dimension of ca. 0.35 mm. It was mounted on a Hilger and Watts Y290 four-circle diffractometer, with c^* a few degrees misaligned from the instrument Φ axis. Unit cell parameters and the orientation matrix were refined by a least-squares technique[7] based on the automatically determined setting angles at room temperature of 12 reflections with 34° < 2θ < 41° (Mo Kα radiation; Zr filter). Values obtained were a = 10.571 (2) Å, b = 11.330 (2) Å, c = 13.469 (2) Å, α = 85.05 (1)°, β = 66.47 (1)°, and γ = 64.24 (1)°. This corresponds to a type I reduced cell[8] with a = 10.571 (2) Å, b = 11.330 (2) Å, c = 13.397 (2) Å, α = 75.16 (1)°, β = 67.19 (1)°, and γ = 64.24 (1)°; the matrix for transformation from initial cell to reduced cell is (−1, 0, 0; 0, −1, 0; −1, 0, 1). Data were collected, reduced, and corrected for absorption on the basis of the initial cell and then transformed to correspond to the reduced cell for all other calculations.

The unit cell volume (1324.6 Å^3) and formula weight (1282.6) give Z = 1 for a density of 1.608 g cm^{-3}. The density was measured as 1.60 ± 0.01 g cm^{-3}. For space group $P1$, no symmetry is imposed on the structure, but for $P\bar{1}$, the dimeric anion must be centrosymmetric. $P\bar{1}$ was assumed and was confirmed by successful structure solution and refinement.

Intensities were collected at room temperature for all independent reflections with 2$\theta \leq$ 45°. A θ–2θ scan was used, with a 1-s count at each of 80 steps of 0.01° for each reflection and a 20-s background count at each end of the scan range. No reflections were sufficiently intense to require the insertion of attenuators into the beam. The data were corrected for Lp factors, absorption, and crystal decay.[9] Absorption corrections were of the Gaussian integration type (μ 20.20 cm^{-1}, 96 grid points), with the crystal approximated by six planar

0020-1669/79/1318-2250$01.00/0